カラーグラス (理論)

Color Glass Condensate (Theory)

渡邉 和宏 (成蹊大学)

Kazuhiro Watanabe (Seikei University)

Tutorial meeting, Osaka Univ., 08/07/2024

Summary, first of all

- "CGC" is a dense gluonic state, that appears at extreme-high energy.
- Any hadrons and nuclei become the CGC state.
- Gluon saturation and its unique phenomena can be described within CGC effective field theory (weak coupling theory).
- Gluon saturation, as an inevitable consequence of Quantum Chromodynamics (QCD), is a scientific truth that we must grapple with in our pursuit of knowledge.
- Hunting saturation by experiments is elusive. We need new experiments, such as ALICE-FOCAL and EIC.

Outline
I. Basics on high energy QCD and CGC
II. Phenomenology and some features of saturation effects

The little-bang on earth

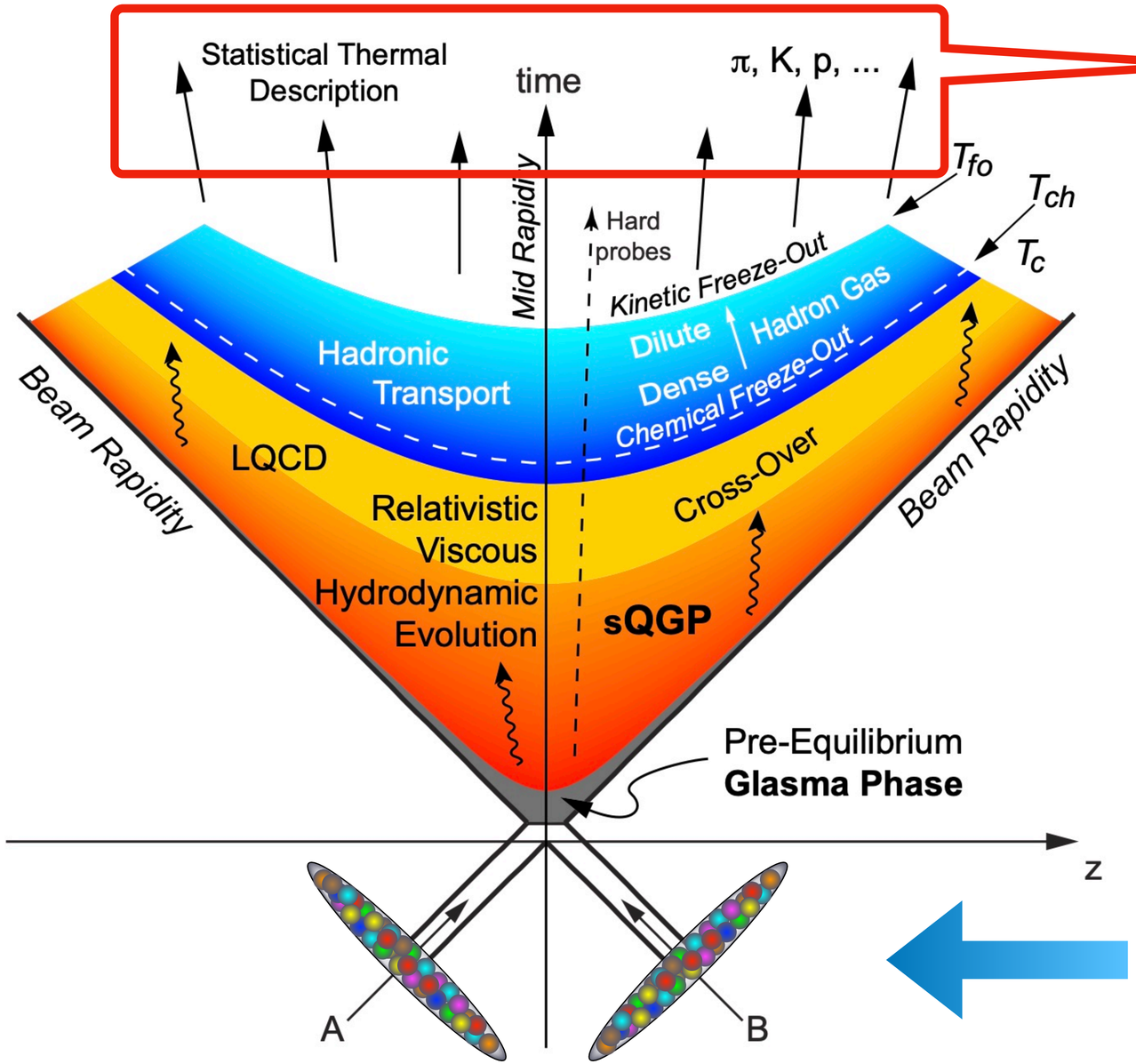

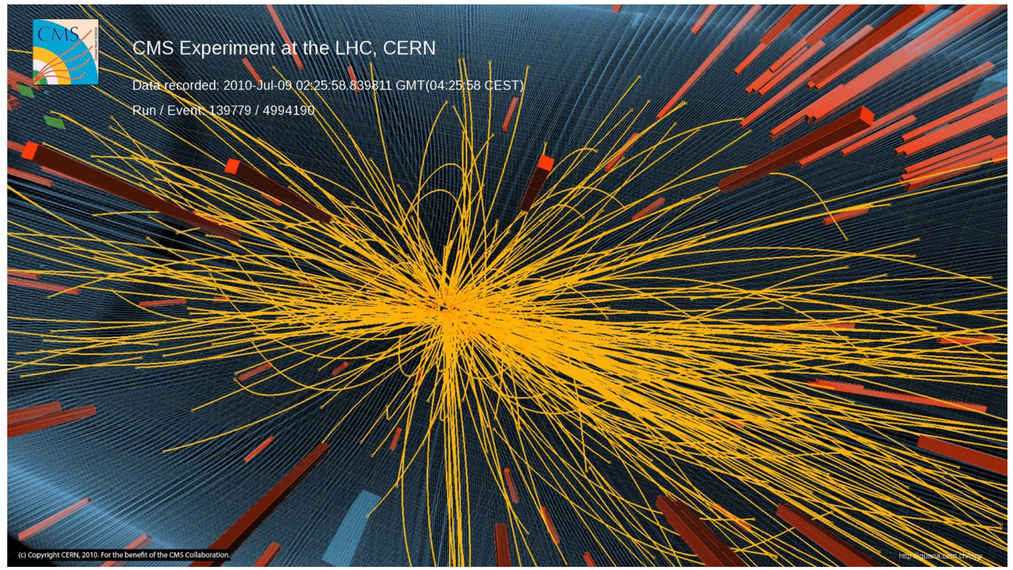

The structure of incoming nuclei (embodied in their wave-functions) affects all physical observables at the last stage!

Figure adapted from http://www.nupecc.org/pub/lrp17/lrp2017.pdf

Why CGC?

CGC should provide crucial input for the space-time evolution of the system after AA collision.

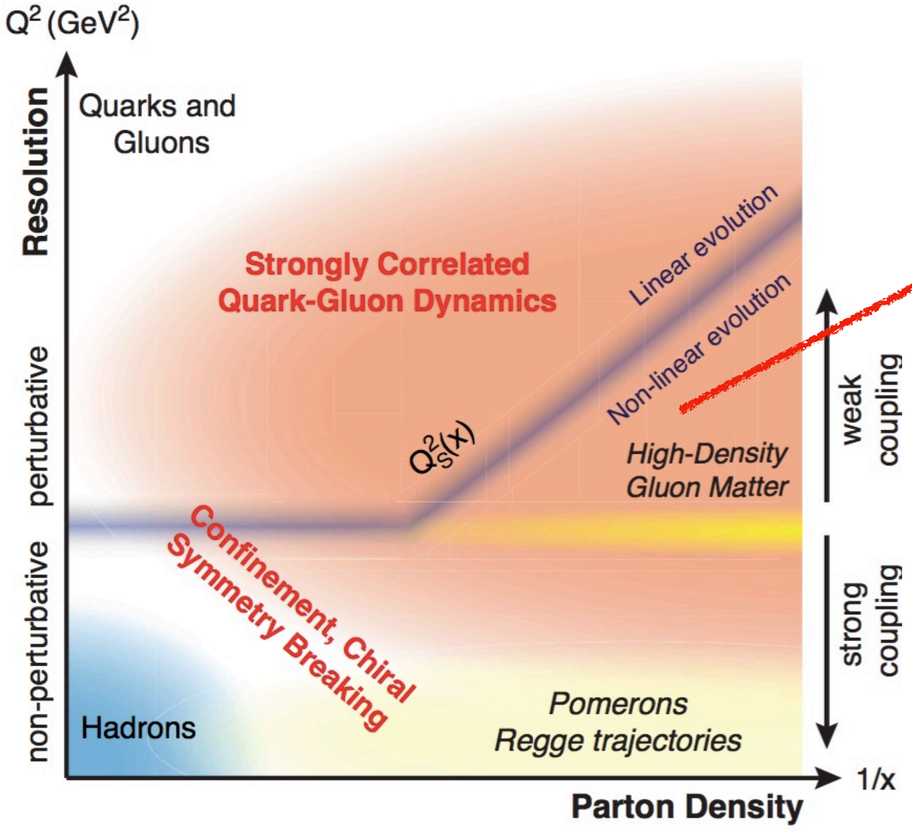

https://u.osu.edu/vishnu/2015/07/22/photon-emission-from-relativistic-heavy-ion-collisions/

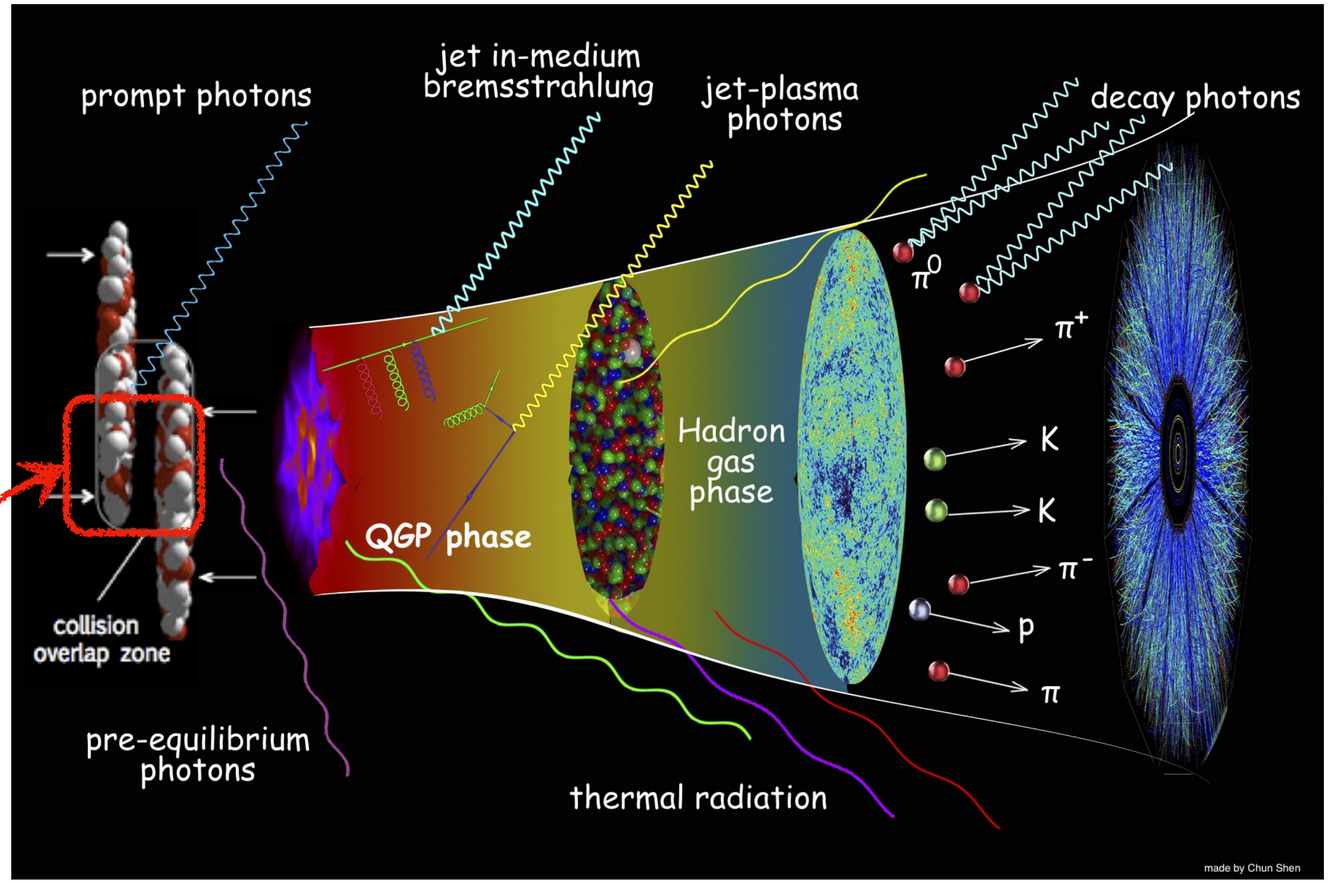

Deep insights into the initial stages are important!

Target kinematic regions

From FPF white paper, J. Phys. G50, no.3, 030501 (2023)

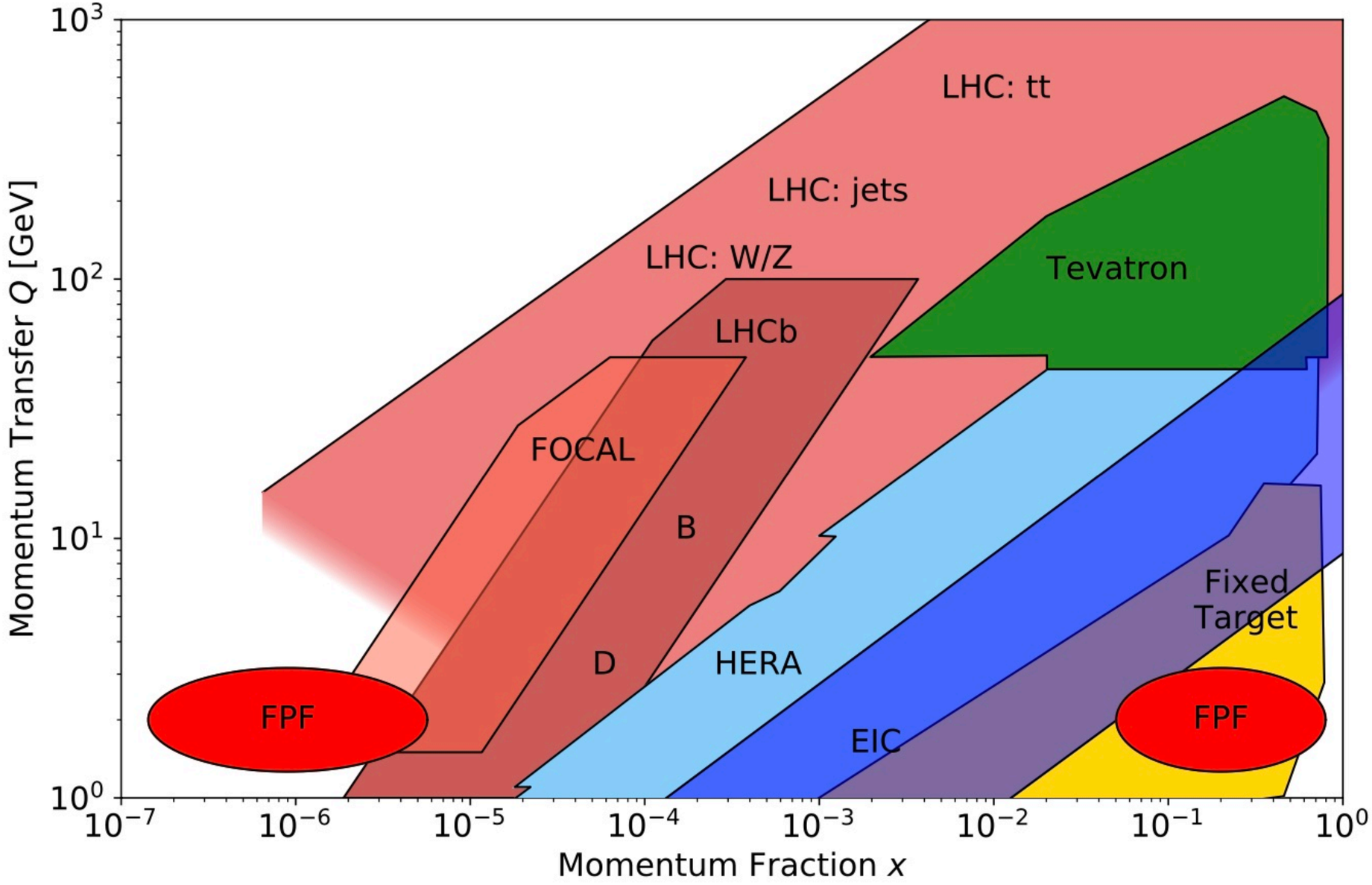

$$x_{\text{target}} \sim \frac{p_\perp}{\sqrt{s}} e^{-y}$$

QCD and Hard probes

$$\mathscr{L}_{\mathrm{QCD}} = \bar{\psi}(iD^{\mu}\gamma_{\mu} - m_q)\psi - \frac{1}{4}F^{a}_{\mu\nu}F^{a\mu\nu}$$

Quarks and **Gluon** carry **color charges**. At short distances $r < 1\mathrm{fm}$, they behave like quasi-free particles.

The Nobel Prize in Physics 2004

Politzer, Gross, Wilczek

Strong coupling constant $\alpha_s = g^2/(4\pi)$

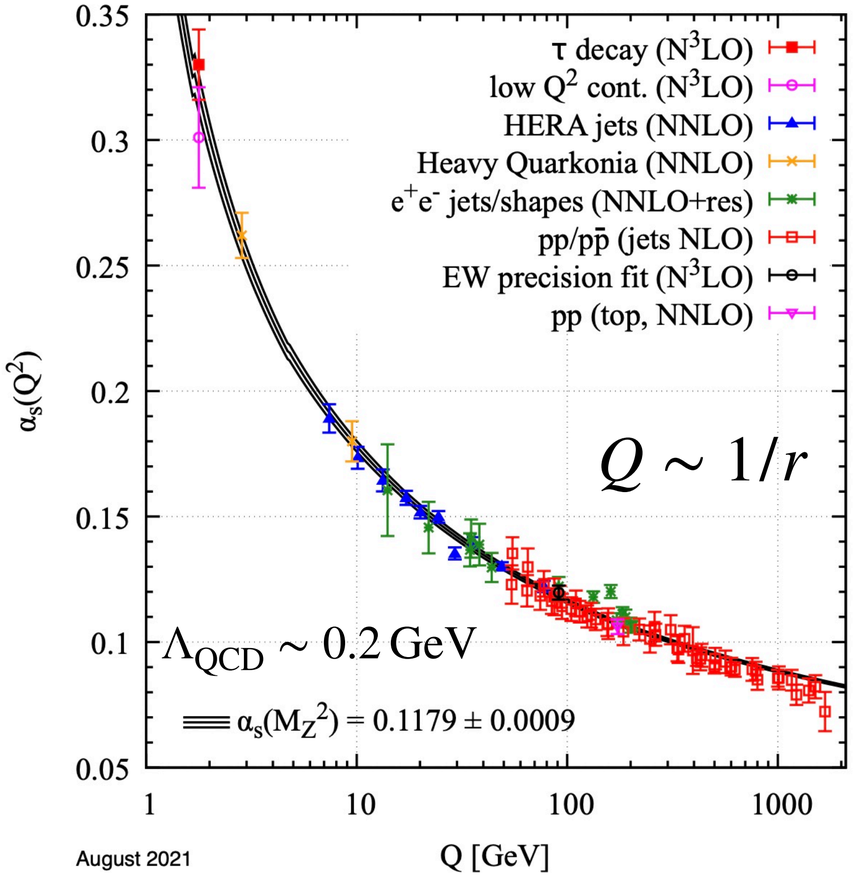

❖ Hard probes ($Q \gg \Lambda_{\mathrm{QCD}}$) enable us to look at quarks and gluons inside hadrons using QCD perturbation theory as $\alpha_s(Q) < 1$.

Hard scale : $Q \gg \Lambda_{\mathrm{QCD}}$

Soft scale : $Q = \mathcal{O}(\Lambda_{\mathrm{QCD}})$

Standard pQCD cannot describe…

S. Acharya *et al.* [ALICE], PLB845, 137730 (2023)

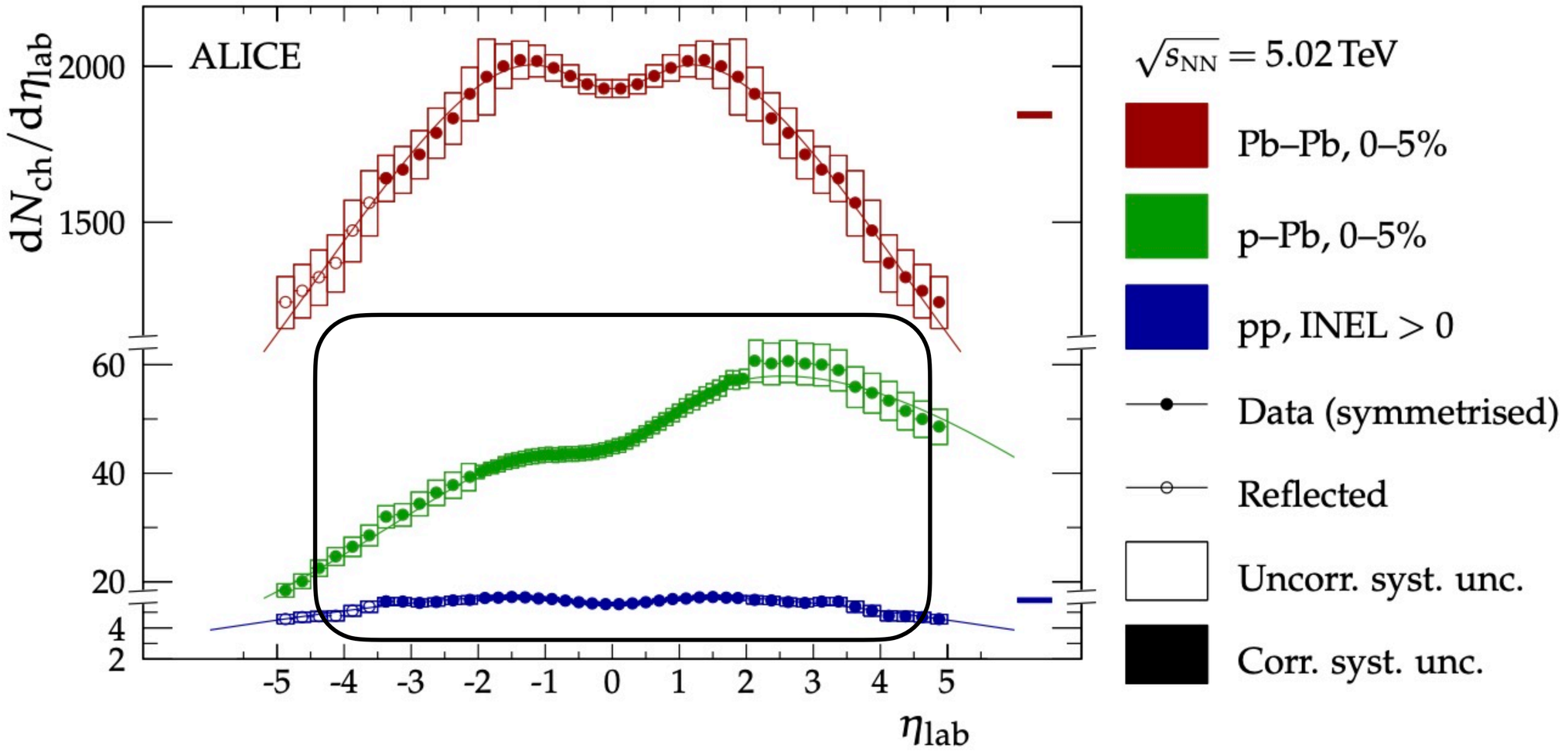

❖ How do we describe bulk particle production of low p_T?

Part I:
Résumé of QCD at high energy

1. Bjorken limit: fixed x with $Q^2, s \to \infty$
2. Regge-Gribov limit: fixed Q^2 with $s \to \infty, x \to 0$
3. Color-Glass-Condensate

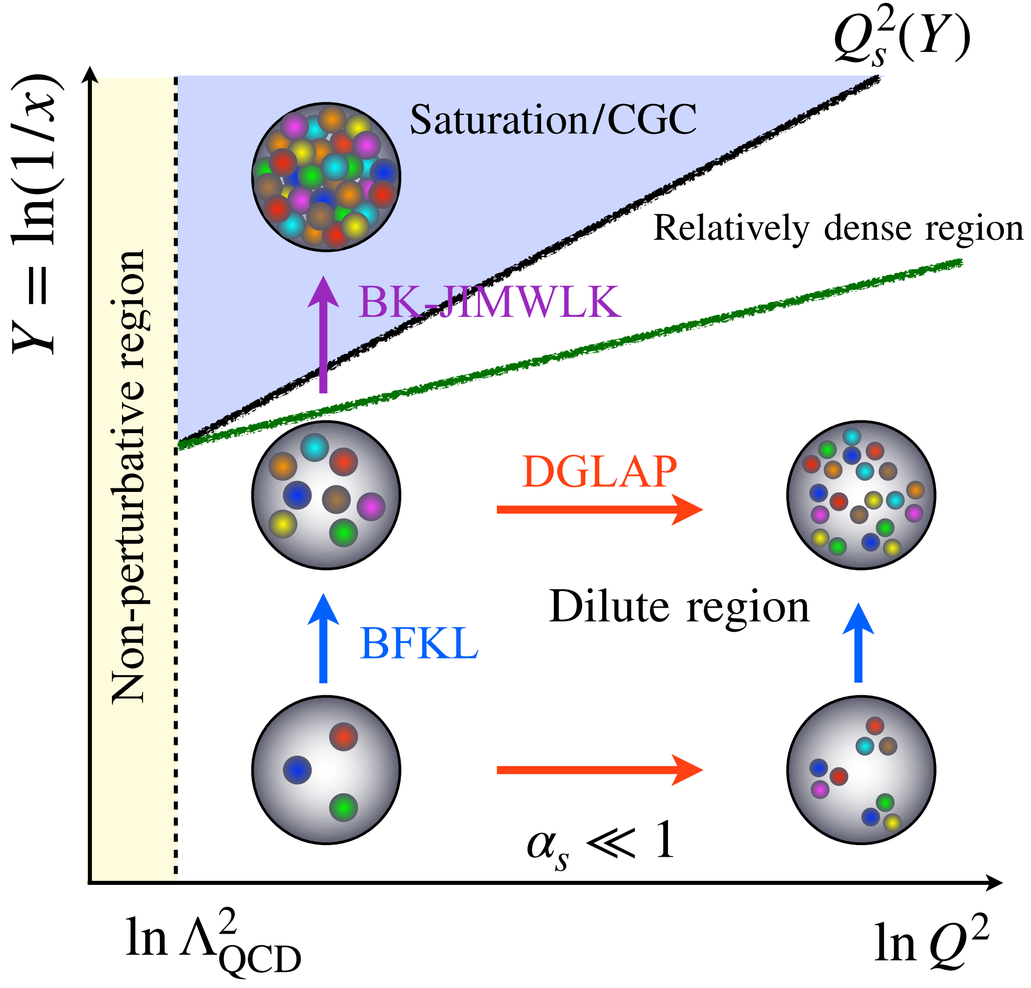

Parton's number density

f : the number density of **partons** with longitudinal momentum fraction x.

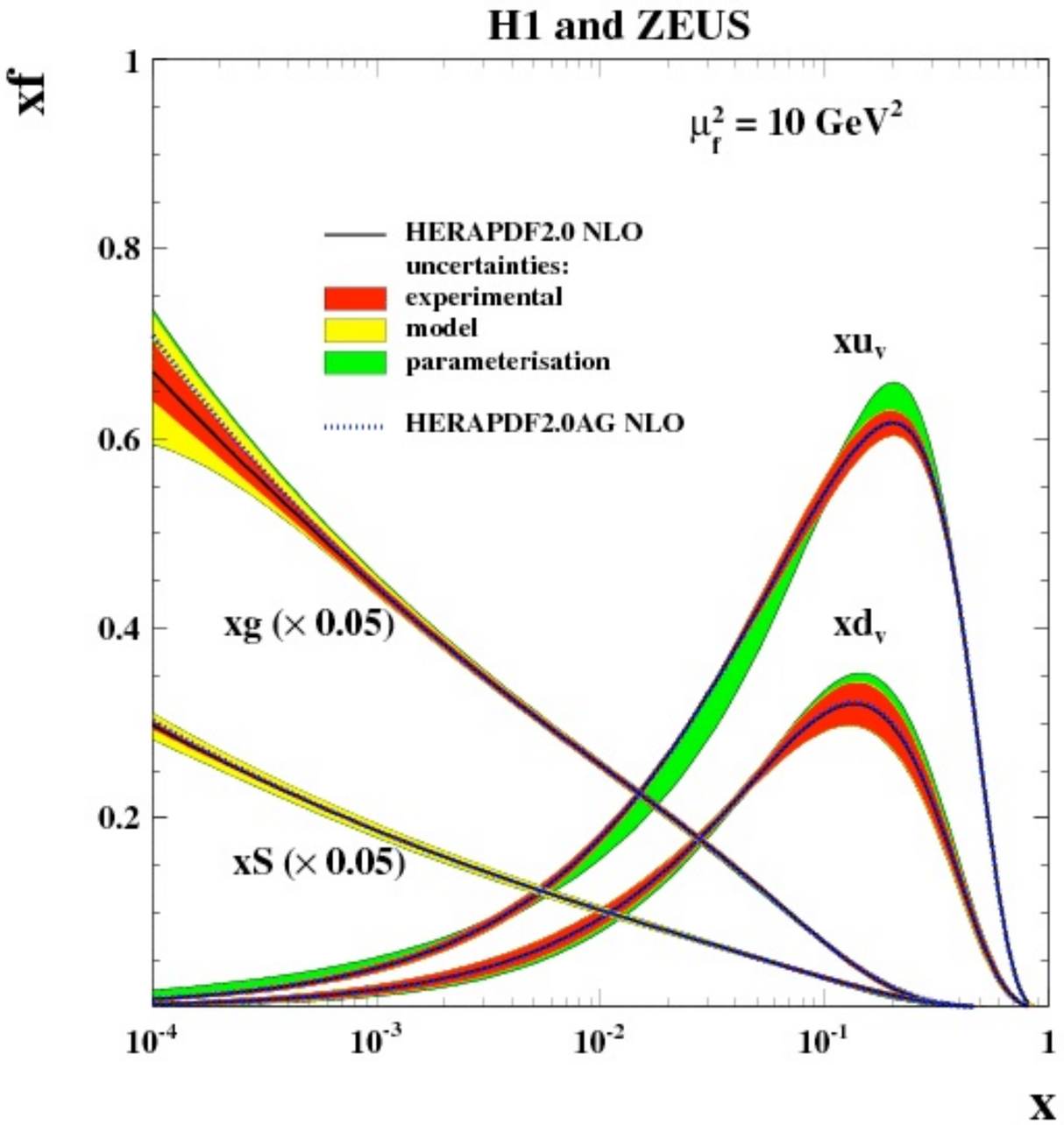

Gluons occupy hadrons at small-x.

Electromagnetic probe

Inclusive DIS ($e + p \to e' + X$) with a large momentum transfer $Q \gg \Lambda_{\mathrm{QCD}}$:

- ❖ dominated by the scattering of the lepton off an active quark/gluon (parton)
- ❖ not sensitive to the dynamics at a hadronic scale $\sim \Lambda_{\mathrm{QCD}} \sim 1/\mathrm{fm}$
- ❖ **QCD factorization** provides the probe to "see" quarks, gluons and their dynamics indirectly:

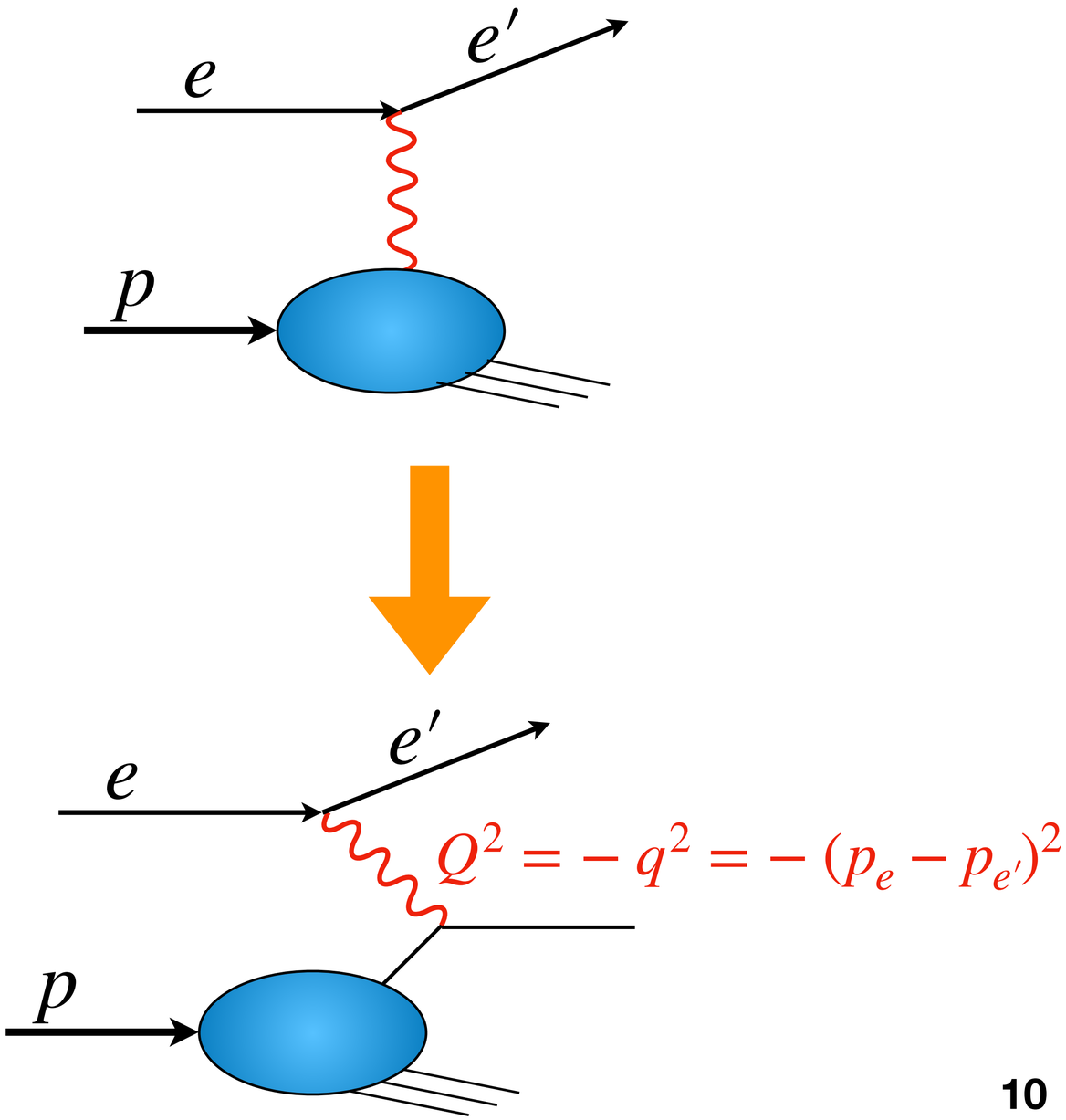

Extracting PDFs

The lepton's energy loss:

$$y = \frac{q \cdot P}{k \cdot P}$$

Center-of-mass energy:

$$s = (P + p)^2$$

Momentum transfer:

$$Q^2 = -q^2$$

Bjorken-x: $x = \frac{P \cdot k}{P \cdot p} \propto \frac{1}{s}$

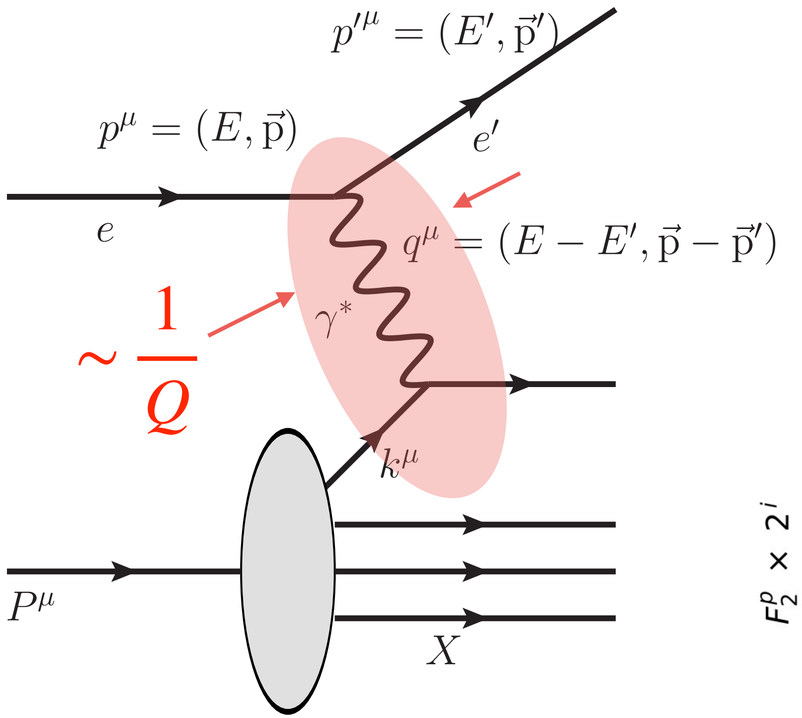

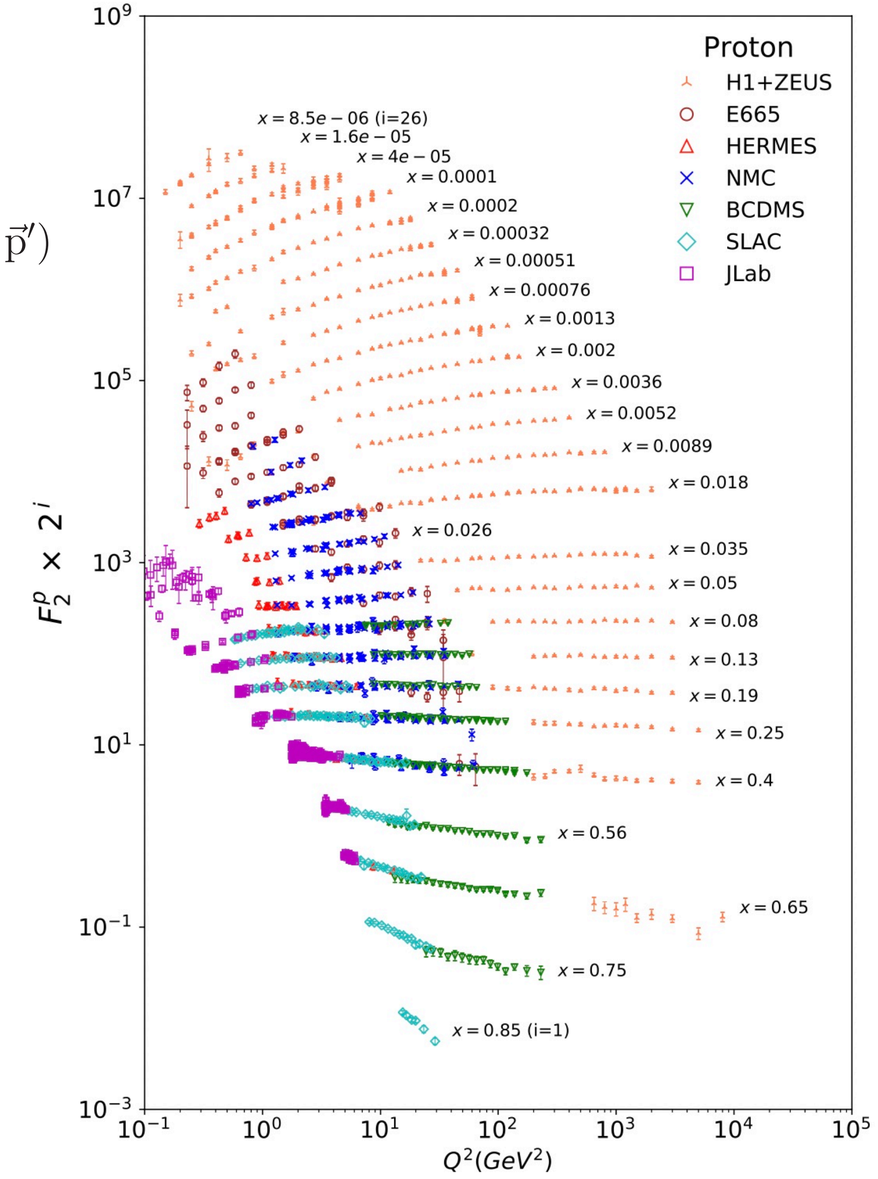

$$\frac{d^2\sigma_{\mathrm{DIS}}}{dxdy} \approx \frac{4\pi\alpha_{\mathrm{EM}}^2}{xyQ^2}\left[(1-y)\,F_2 + y^2 x F_1\right]$$

Structure functions $F_i \approx \sum_a C_i^a \otimes f_a$ ← Global data fitting

Perturbatively calculable

Reference frame

- Hadron rest frame: $P^\mu = (M,0,0,0)$
- Infinite momentum frame (IMF): $P \gg M \Longrightarrow P^\mu = (P,0,0,P)$

In IMF, partonic picture is manifest. PDFs are number densities.

- Light-cone coordinate: $x^\pm = (t \pm z)/\sqrt{2}$
- Light-cone momentum: $p^\pm = (E \pm p_z)/\sqrt{2}$
- Rapidity: $y = \frac{1}{2}\ln\left(\frac{p^+}{p^-}\right)$
- "Longitudinal" momentum fraction: $x = k^+/P^+$

In IMF, $P^\mu \to (P^+,0^-,0_\perp)$

If $P^\mu = (P,0,0,-P)$, $P^\mu \to (0^+,P^-,0_\perp)$

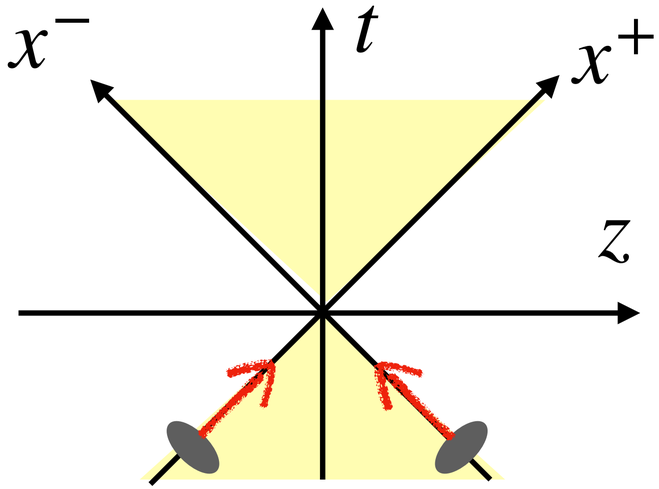

We will discuss scatterings in the light-cone coordinate.

Two characteristic scales

Image resolution

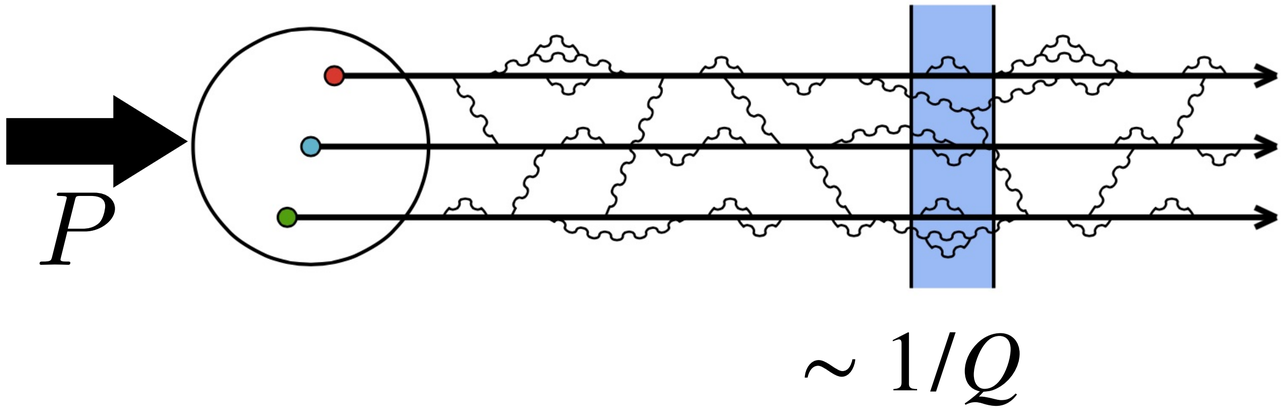

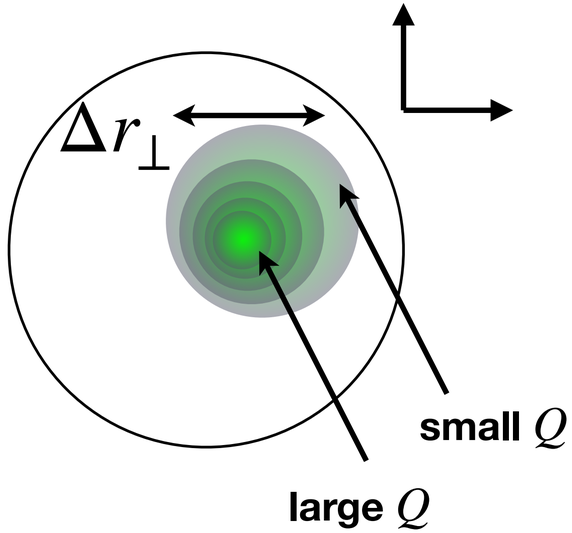

Localized probe $\Delta r_\perp \propto 1/Q$: spatial resolution in transverse plane

Exposure time

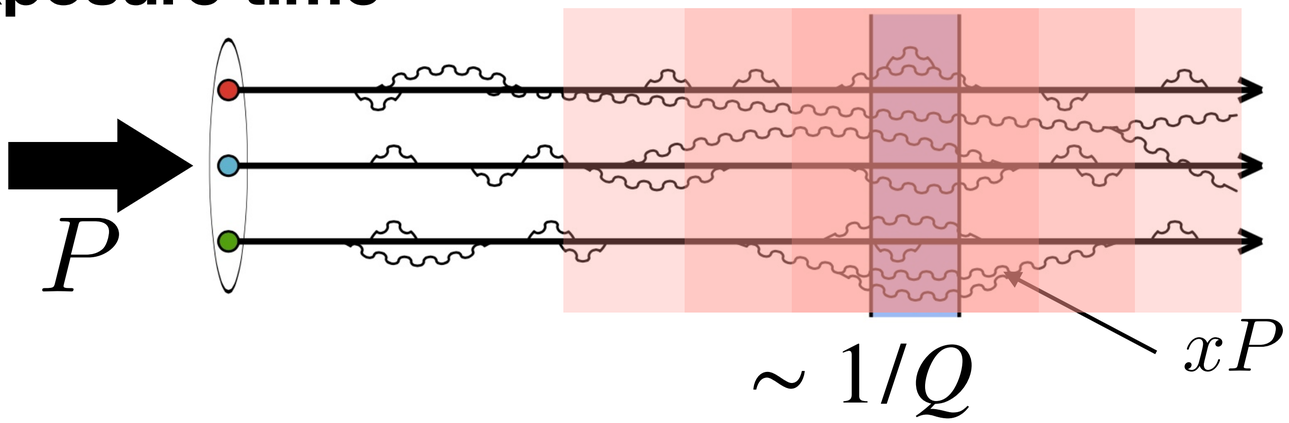

Ioffe time $\Delta t \propto 1/x$: fluctuation in longitudinal direction

lifetime of a parton in IMF:

$$\Delta t \sim \Delta x^+ \sim k^- = \frac{k_T^2}{2k^+} = \frac{k_T^2}{2xP^+}$$

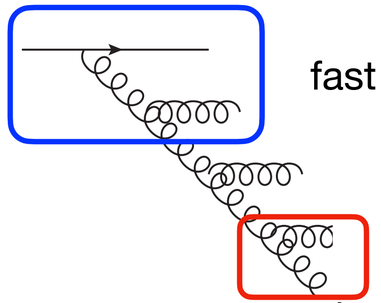

fast gluon: long lifetime

slow gluon: shot lifetime

Scale evolution of PDFs in Bjorken limit

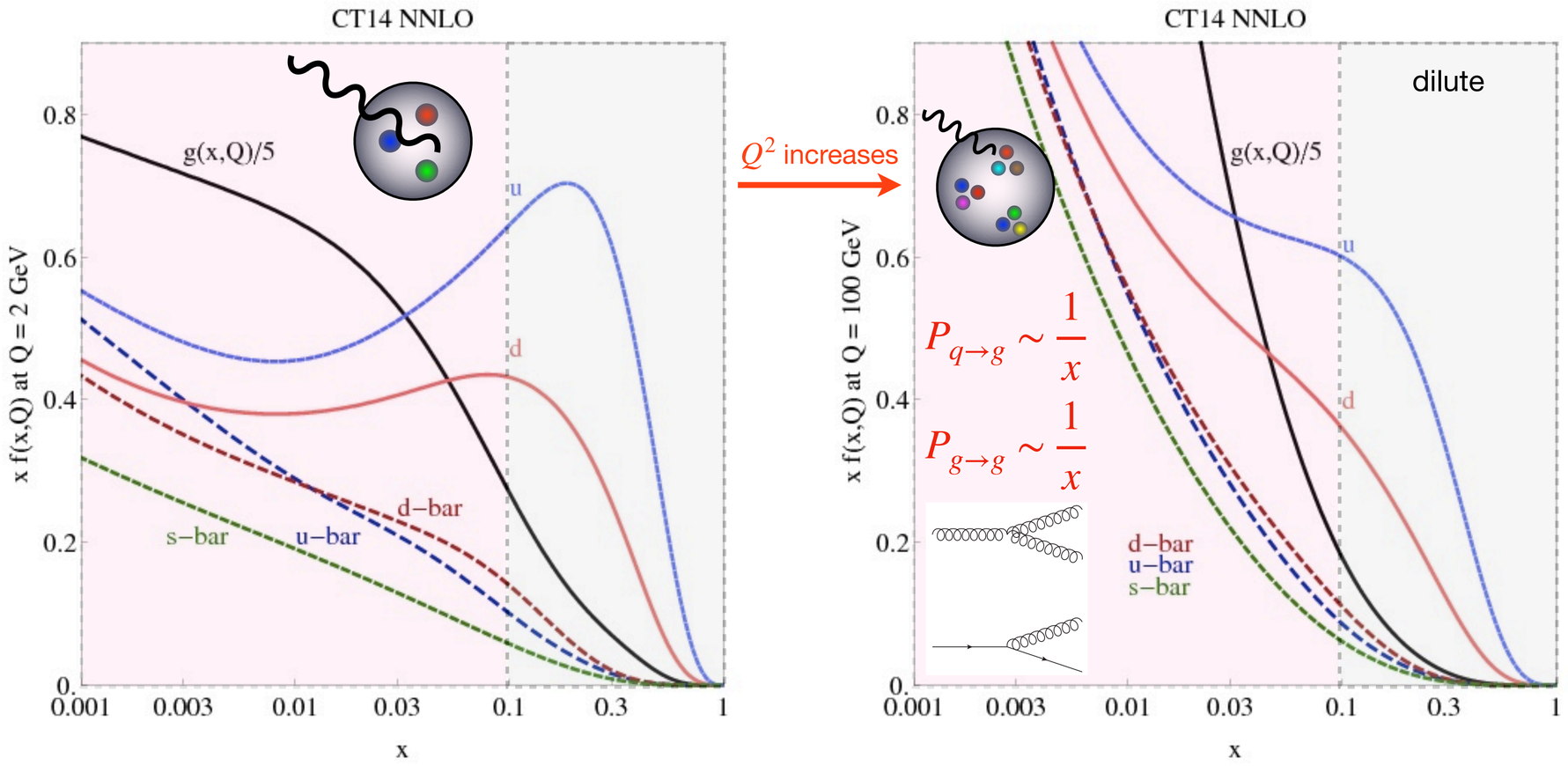

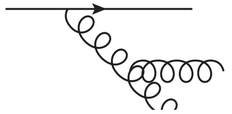

- DGLAP equations resum $\alpha_s \ln(Q^2)$-type enhanced corrections. (x is fixed)
- The double logs approximation of DGLAP equations at small-x can be solved analytically: $xf_g \sim e^{\sqrt{\ln(1/x)\ln(Q^2)}}$

$$\alpha_s \int_{\Lambda^2}^{Q^2} \frac{dk_T^2}{k_T^2} = \alpha_s \ln(Q^2/\Lambda^2)$$

Regge-Grobov limit

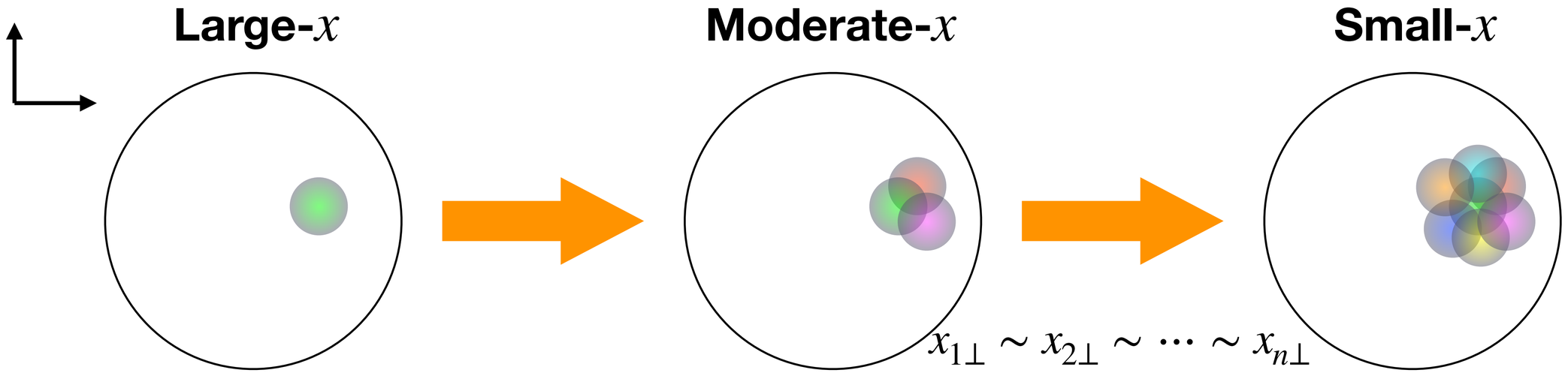

- The number of partons increases due to the increased longitudinal phase space as $x \to 0$.
- The radiated gluons are of the same transverse size ($x_\perp \sim 1/Q$).
- BFKL equation resums large $\ln(1/x)$-type corrections.
- Hadron/nucleus becomes dense. A quasi-free parton picture is not so useful.

Balitsky-Fadin-Kuraev-Lipatov evolution at small-x

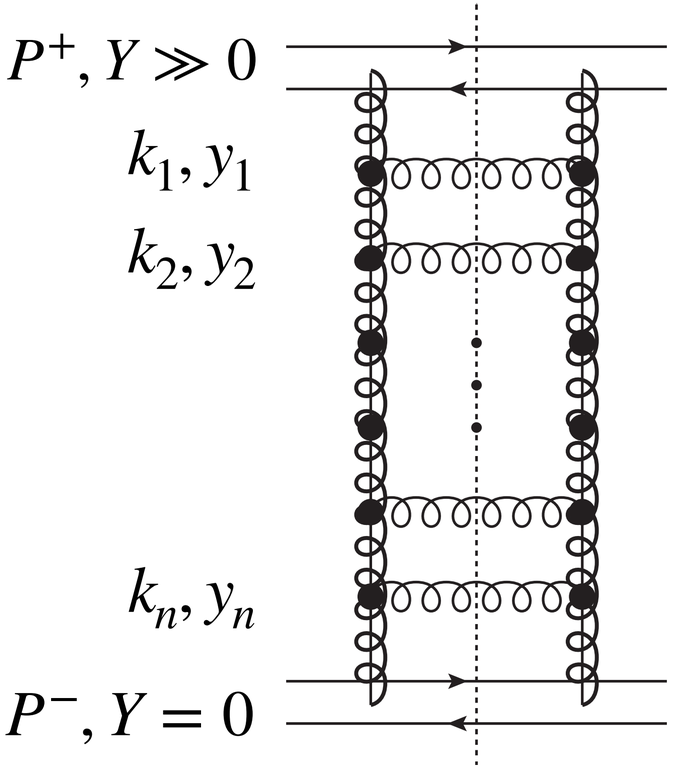

Unintegrated gluon distribution $\phi(x, Q^2) = \partial x f_g(x, Q^2)/\partial Q^2$ obeys BFKL equation:

$$\frac{\partial \phi(x, k_\perp)}{\partial \ln(1/x)} = \frac{\alpha_s N_c}{\pi^2} \int \frac{d^2 q_\perp}{(k_\perp - q_\perp)^2} \left[\phi(x, q_\perp) - \frac{k_\perp^2}{2q_\perp^2} \phi(x, k_\perp) \right]$$

$$\phi(x, k_\perp) \sim e^{(\alpha_P - 1)Y} \sim \left(\frac{1}{x} \right)^{\alpha_P - 1}$$

- Intercept of the BFKL perturbative pomeron: $\alpha_P - 1 = \frac{4\alpha_s N_c}{\pi} \ln 2 \sim 0.79$
- The analysis of experimental data showed $\sigma_{tot} \sim s^{0.1}$ (soft pomeron)

A. Donnachie and P. V. Landshoff, PLB727, 500-505 (2013) [erratum: PLB750, 669-669 (2015)]

DIS in Dipole frame at high energy

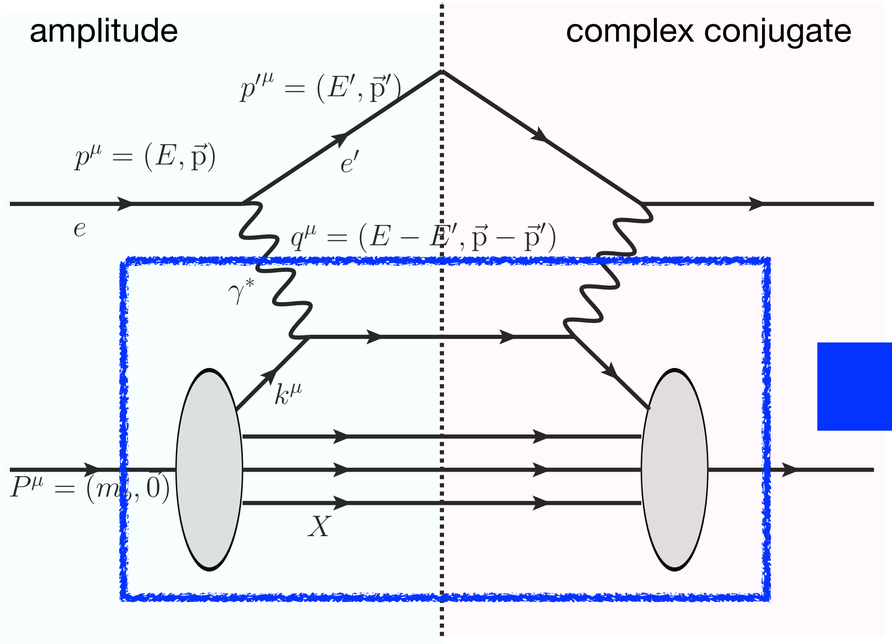

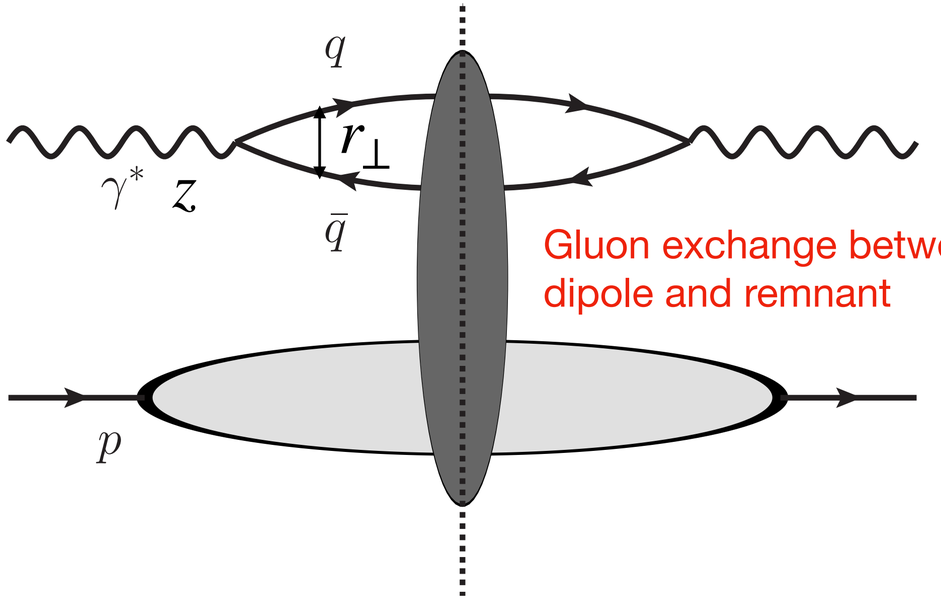

Gluon exchange between dipole and remnant

- Both the proton and photon move along the z-axis in opposite directions.
- The standard partonic picture is no longer valid.

Factorization at high s

$$\sigma_{tot}^{\gamma^* A}(x, Q^2) = \int d^2 r_\perp \int_0^1 dz \left| \Psi^{\gamma^* \to q\bar{q}}(r_\perp, z, Q^2) \right| \hat{\sigma}_{tot}^{q\bar{q}A}(r_\perp, x)$$

QED part: calculable in light-cone perturbation theory

QCD part: the dipole amplitude

BFKL evolution in Dipole frame

$$Y = \ln(z_1/z_0)$$

Mueller's dipole model: Al. Mueller (1994)

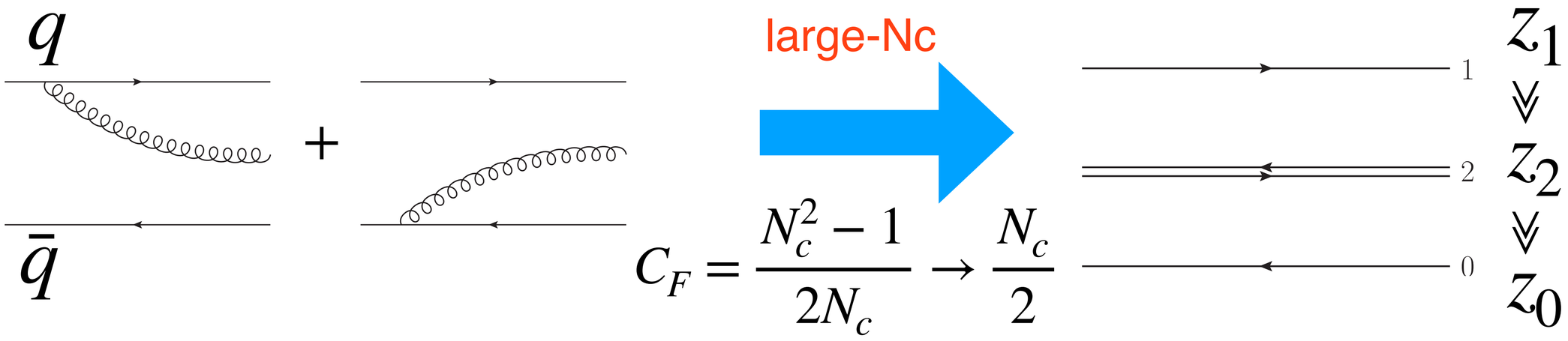

Two daughter dipoles (Real)

$$\frac{\partial}{\partial Y} N(x_{10}, Y) = \frac{\alpha_s N_c}{2\pi^2} \int d^2x_2 \frac{x_{10}^2}{x_{20}^2 x_{21}^2} \left[N(x_{12}, Y) + N(x_{20}, Y) - N(x_{10}, Y) \right]$$

Parent dipole

Absorption (Imaginary)

- Problem 1: $\sigma_{\rm BFKL} \sim s^{\alpha_P - 1}$ can violate a unitarity bound $\sigma \propto \ln^2 s$.
- Problem 2: because of the diffusion of the ladder, BFKL could go to the IR regime.

Gluon saturation

Gribov, Levin and Ryskin, Phys. Rept. 100, 1 (1983)
Mueller and Qiu, NPB268, 427 (1986), Qiu, NPB291, 746 (1987)

Modified DGLAP (GLV-MQ) equation at small-x:

$$\frac{\partial x f_g}{\partial \ln(1/x)\,\partial \ln \mu^2} = \frac{\alpha_s N_c}{\pi}\left(x f_g\right) - \frac{1}{\mu^2}\frac{\alpha_s^2 N_c \pi}{2 C_F S_\perp}\left(x f_g\right)^2$$

- Gluon recombination slows down the small-x evolution.
- The nonlinear term is a higher twist correction, suppressed by $1/\mu^2$, but remains to be significant even at high μ^2.
- All-twist contributions are equally important.

$$\frac{\partial x f_g}{\partial \ln(1/x)\,\partial \ln \mu^2} = 0 \longrightarrow Q_s^2 \sim \mu^2 = \frac{\alpha_s \pi^2 x f_g}{2 C_F S_\perp}$$

Saturation scale

$$x f_g(x, Q^2) = \int^{Q^2} dk_\perp^2\, \phi(x, k_\perp)$$

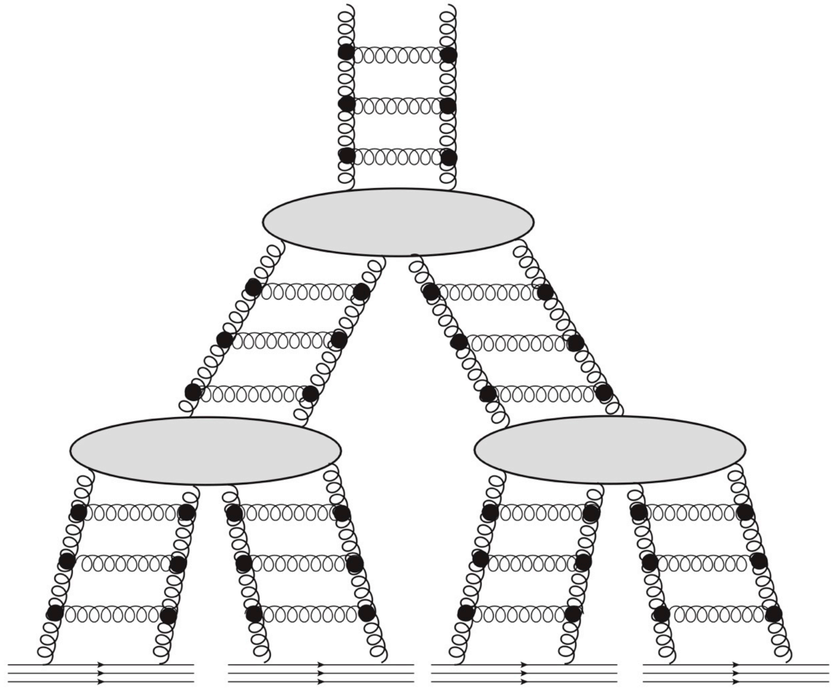

large occupation number : strong field

$$N_g \sim \frac{x f_g}{S_\perp Q_s^2} \sim \frac{1}{\alpha_s}$$

Geometric Scaling from HERA

DIS total cross section ($\sigma_{tot}^{\gamma^* p}$) is the function of only one dimensionless variable τ:

$$\tau \sim \frac{Q^2}{Q_0^2}\left(\frac{x}{x_0}\right)^{\lambda}$$

$$\lambda = 0.288,\ x_0 = 3.04 \times 10^{-4}$$

- The scaling is seen at $x \leq 0.01$ even at high Q^2.
- $\lambda \sim 0.3$: a slower x-dependence and consistent with running coupling BK eq.

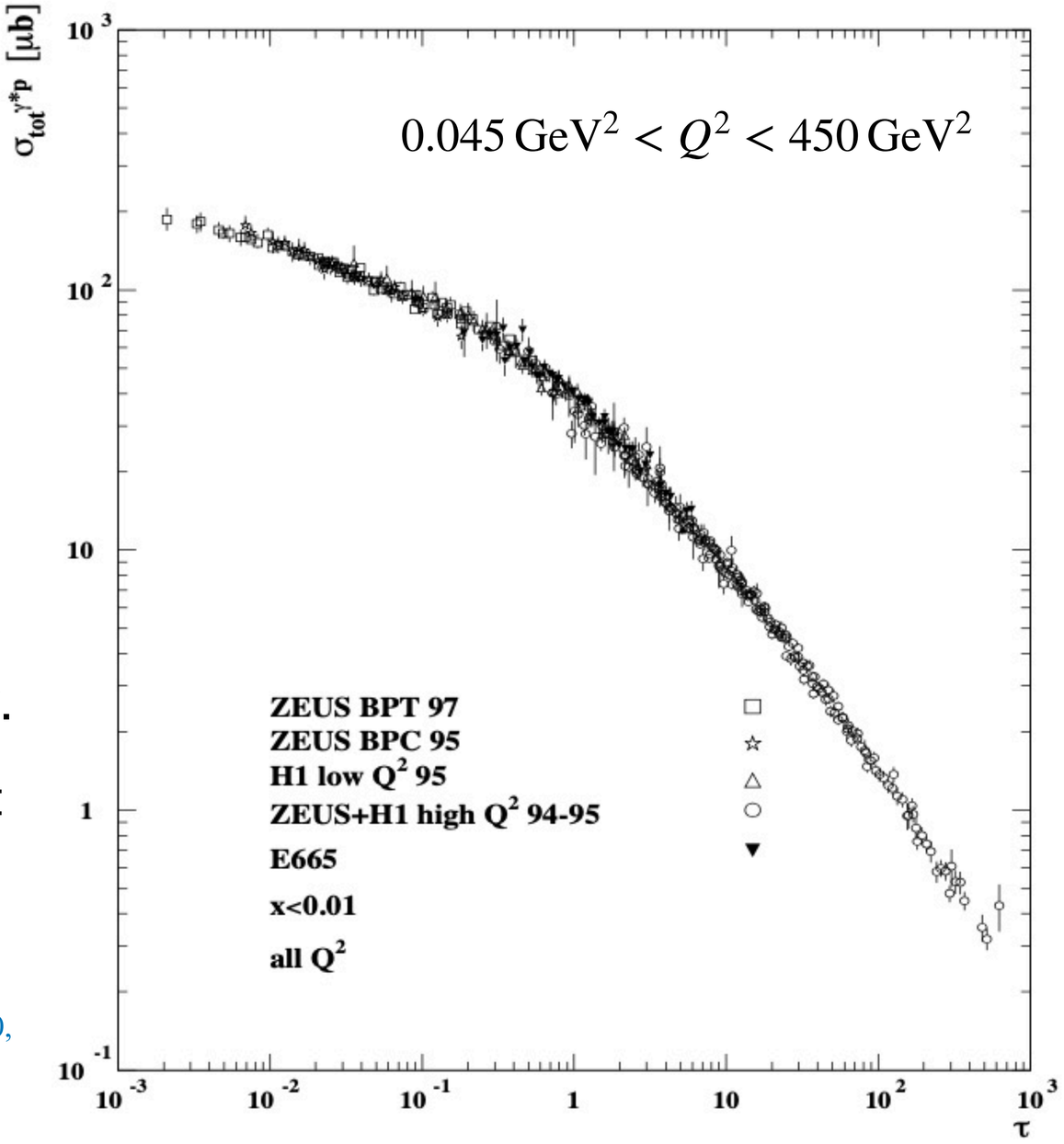

Golec-Biernat and Wusthoff, PRD59, 014017 (1998), PRD60, 114023 (1999)
Stasto, Golec-Biernat and Kwiecinski, PRL86, 596 (2001)

Color Glass Condensate (CGC): Gluonic matter

Color: Quarks and gluons carry color charges.

Glass: Small-x gluons evolve slowly. A loose analogy to “Spin Glass”.

Condensate: High gluon density. A loose analogy to “Bose Condensate”.

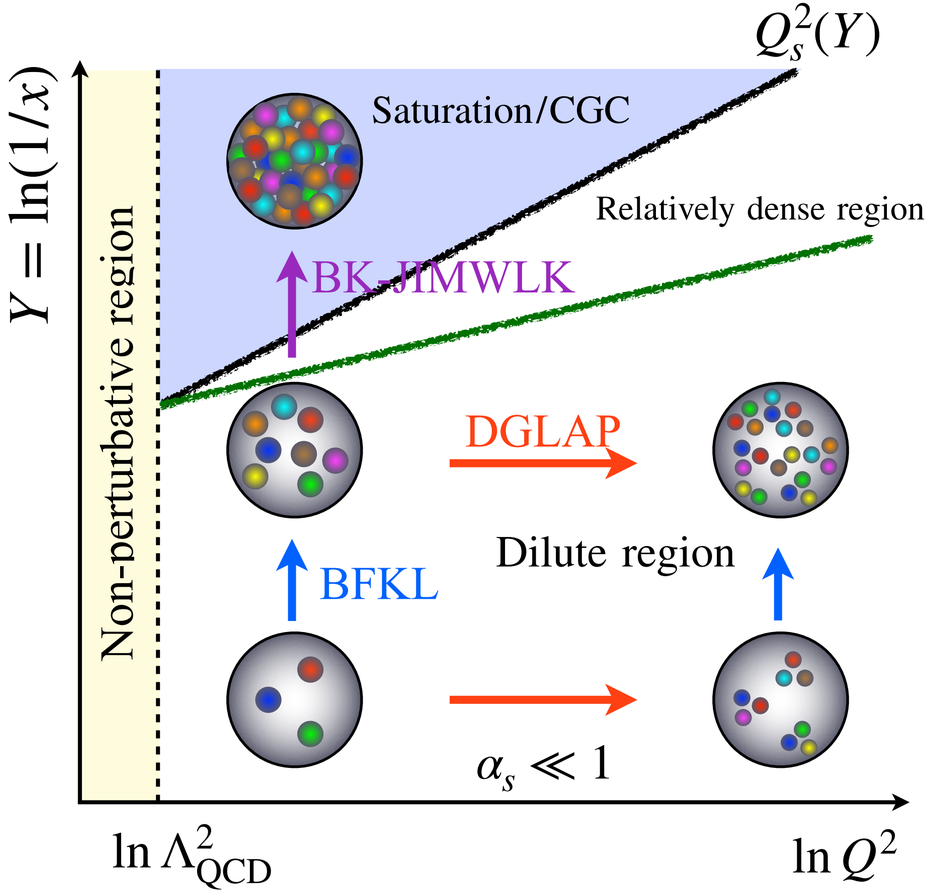

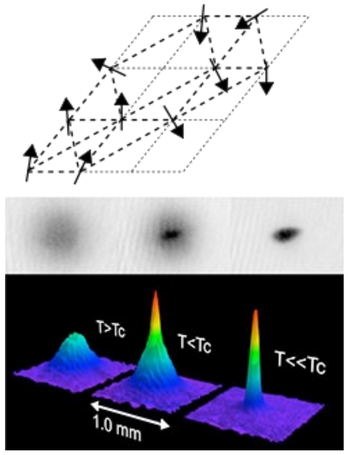

https://coldatomlab.jpl.nasa.gov/sciencebackground/

- Gluons per unit area: $\rho \propto \dfrac{Axf_g}{\pi R_A^2}$
- Recombination: $\sigma_{gg\to g} \propto \dfrac{\alpha_s}{Q^2}$
- Saturation starts when $\rho\sigma_{gg\to g} \sim \mathcal{O}(1)$ leading to $Q_s^2 \propto A^{1/3}x^{-\lambda} \gg \Lambda^2_{\rm QCD}$
- Weak-coupling theory ($\alpha_s(Q_s^2) \ll 1$) describes bulk soft particle production: **new paradigm**.

Wilson line: new degrees of freedom

Interaction with background gauge field in Eikonal approximation: gauge (phase) rotation

- The quark's trajectory inside the shockwave can be frozen: Eikonal approximation.
- The interaction of the quark with the shockwave (gauge rotation) will be described by a gauge factor ordered along this segment of a straight line → Wilson line

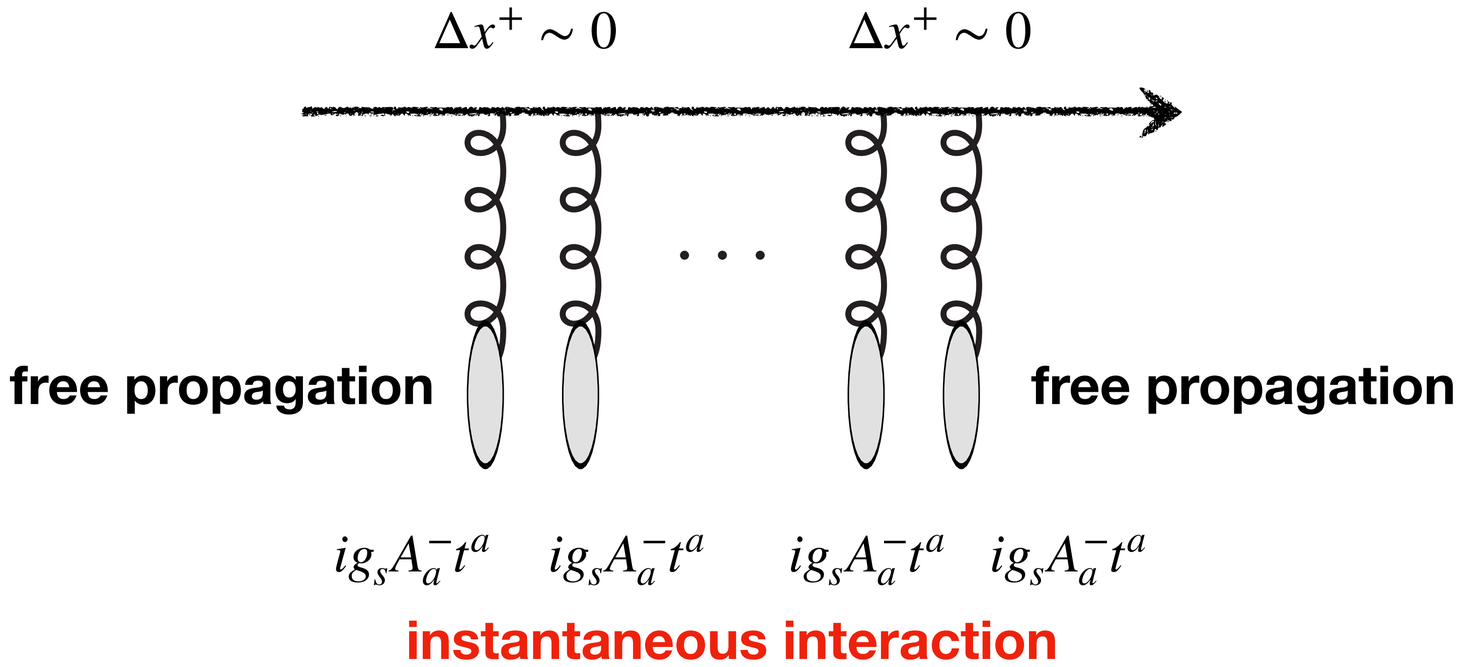

Quark and gluon receive different gauge rotations (fundamental or adjoint reps.) when traversing the shockwave.

$$U_r = \mathscr{P} \exp\left[ig_s \int_{-\infty}^{\infty} \mathrm{d}x^+ A_a^-(x^+, r) t^a \right]$$

Shockwave approximation

Background field becomes a shockwave "wall"

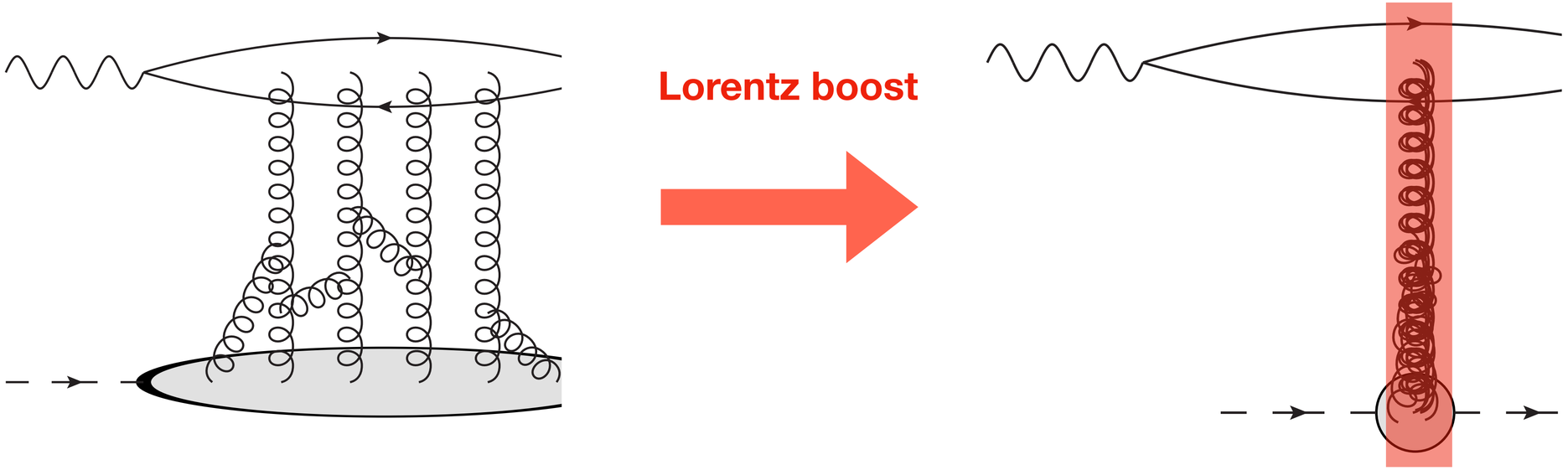

- The shockwave is very thin: coherent interaction
- The quark has no time to deviate in the transverse direction.

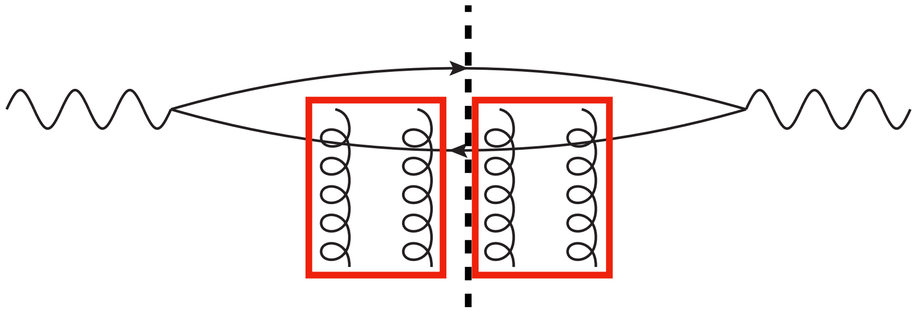

$$S(r_\perp = x_{01}) = \frac{1}{N_c}\langle \mathrm{Tr}\left[U^\dagger(x_0)U(x_1)\right]\rangle$$

Dipole amplitude and saturation

$$S(r_\perp = x_{01}) = \frac{1}{N_c}\langle \mathrm{Tr}\left[U^\dagger(x_0)U(x_1)\right]\rangle$$

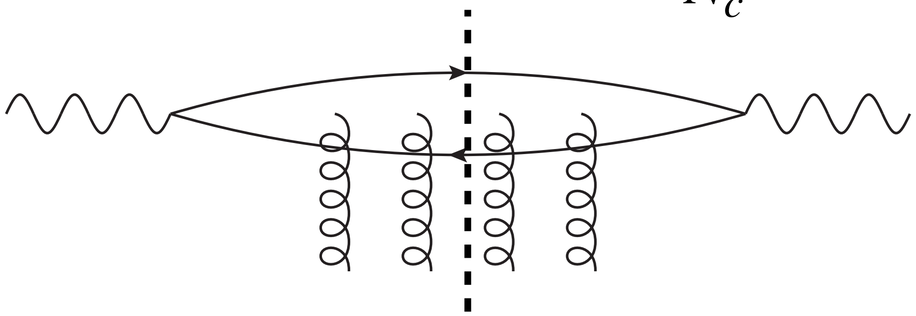

$$\sigma_{q\bar{q}N}(r_\perp, x) = 2\int d^2b_\perp N(r_\perp, x) = \sigma_0\left[1 - e^{-r_\perp^2 Q_s^2(x)}\right]$$

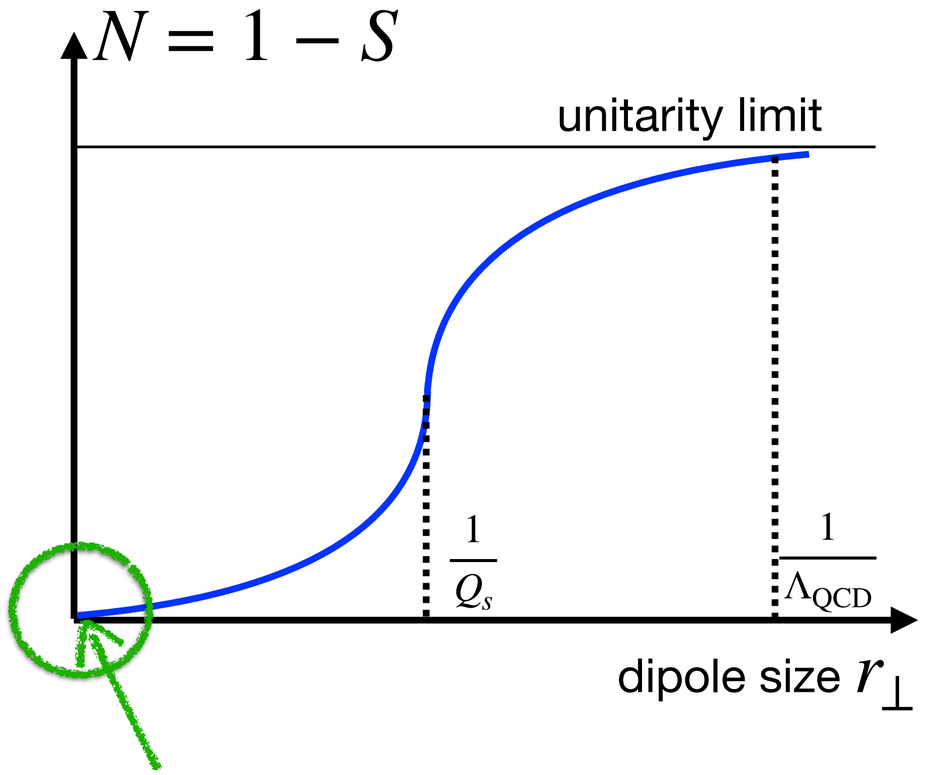

- Bjorken frame (IMF): Saturation is the limit of parton's number density.
- Dipole frame: Patonic picture is no longer manifest. Saturation is the unitarity limit for scatterings.

As $r_\perp \to 0$, the color charges of the quark and the antiquark cancel each other

$\Longrightarrow$ the disappearance of interactions with the target (Color Transparency)

Color Glass Condensate Effective Field Theory

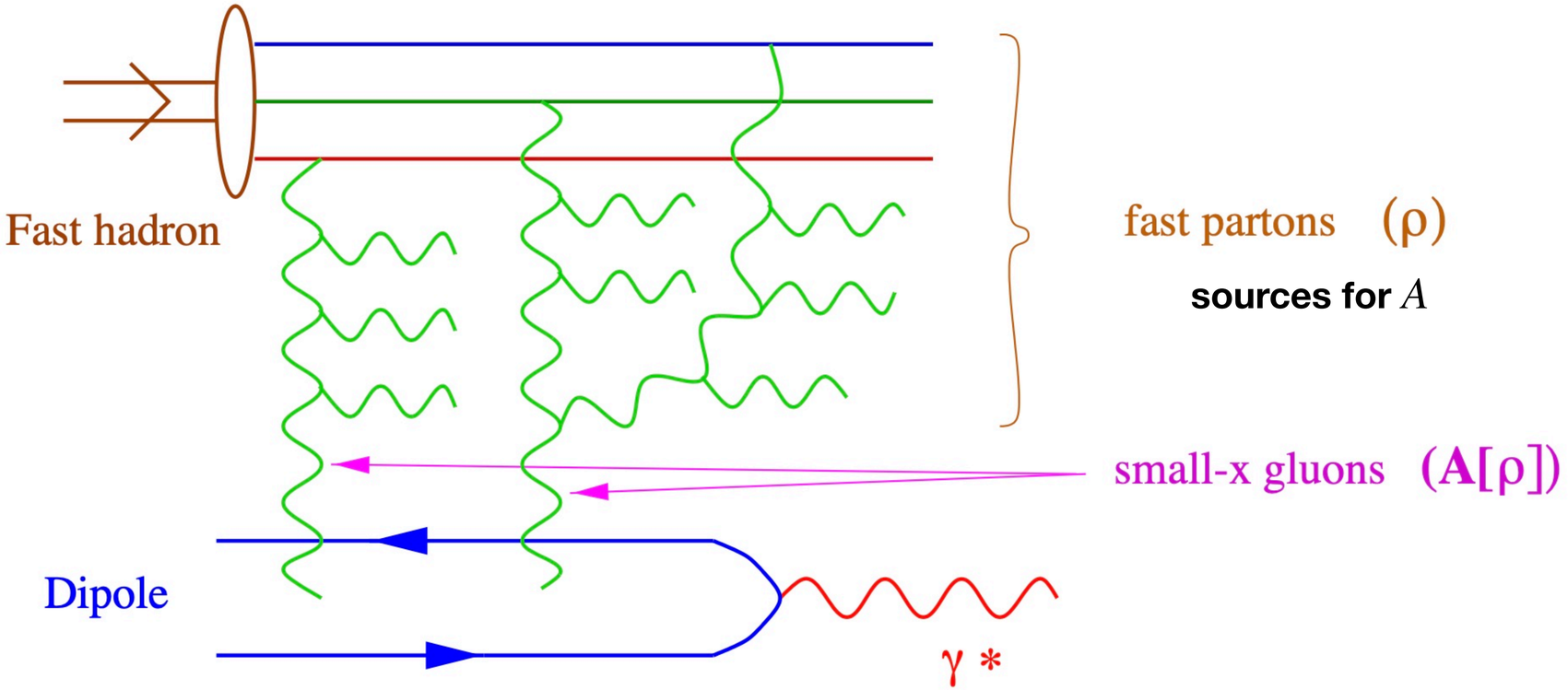

- Static and strong $(1/g)$ color charge ρ
- Universal statistical distribution $W[\rho]$ (c.f. PDFs in Bjorken limit)
- Color current $J_a^\mu = \delta^{+\mu}\rho^a$

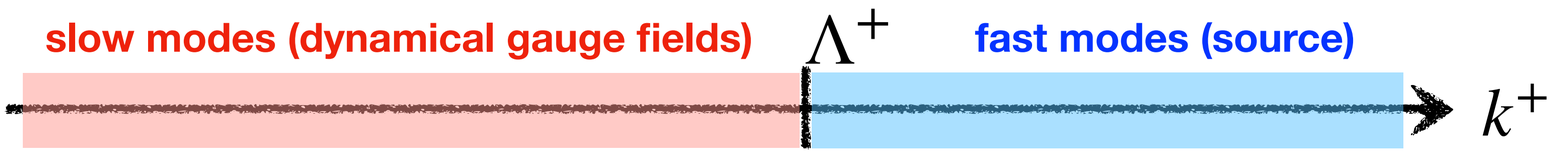

JIMWLK renormalization group equation describes the separation between fast modes ($k^+ > \Lambda^+$) and slow modes ($k^+ < \Lambda^+$).

Dynamical gauge field

- Hadron wave function = collection of static color sources ρ (classical random variable)
- Hard and soft modes are coupled via Yang-Mills equations at LO (classical equations of motion):

$$[\mathscr{D}_\mu, F^{\mu\nu}] = J^\nu \quad \text{with} \quad J^\nu = \delta^{+\nu}\rho$$

The occupation numbers are large, so the generated classical fields are strong: $A \sim \frac{1}{g}$

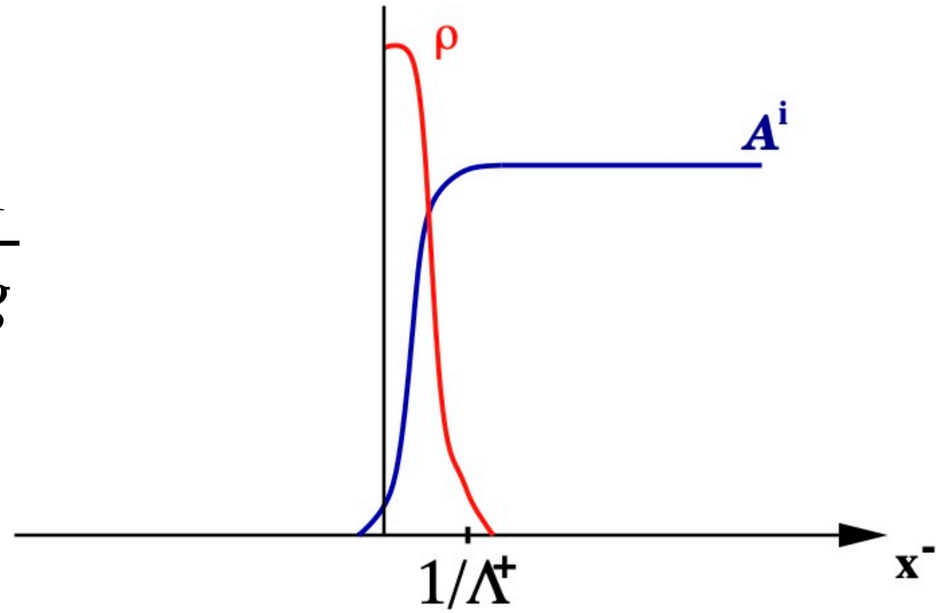

CGC expectation value

$$\langle \mathcal{O} \rangle_{\Lambda^+} = \frac{\int [\mathscr{D}\rho] W_{\Lambda^+}[\rho] \mathcal{O}[\rho]}{\int [\mathscr{D}\rho] W_{\Lambda^+}[\rho]}$$

n-point Wilson line correlators

- ✓ gauge invariant
- ✓ probability of a configuration ρ
- ✓ in the saturation regime, $\rho = \mathcal{O}(1/g)$
- ✓ normalization: $\int [\mathscr{D}\rho] W_{\Lambda^+}[\rho] = 1$

The requirement that physical quantities (the expectation value of the operator) do not depend on the choice of the cutoff Λ^+, leading to the Jalilian–Marian–Iancu–McLerran–Weigert–Leonidov–Kovner (JIMWLK) equation for $W_{\Lambda^+}[\rho]$:

$$\frac{\partial W_Y[\rho]}{\partial Y} = -\mathscr{H}_{\text{JIMWLK}}\, W_Y[\rho]$$

resums all powers of $\alpha_s Y$

$$\rightarrow \quad \frac{\partial \langle \mathcal{O} \rangle_Y}{\partial Y} = \left\langle \mathscr{H}_{\text{JIMWLK}}\, \mathcal{O} \right\rangle_Y$$

Customary notation:

$\Lambda^+ \leftrightarrow x = \Lambda^+/P^+$

$x \leftrightarrow Y = \ln(1/x)$

B-JIMWLK evolution

Let us consider S-matrix $\mathcal{O} = S(x_{10}) = \frac{1}{N_c}\mathrm{Tr}[U^\dagger(x_1)U(x_0)]$ as an example:

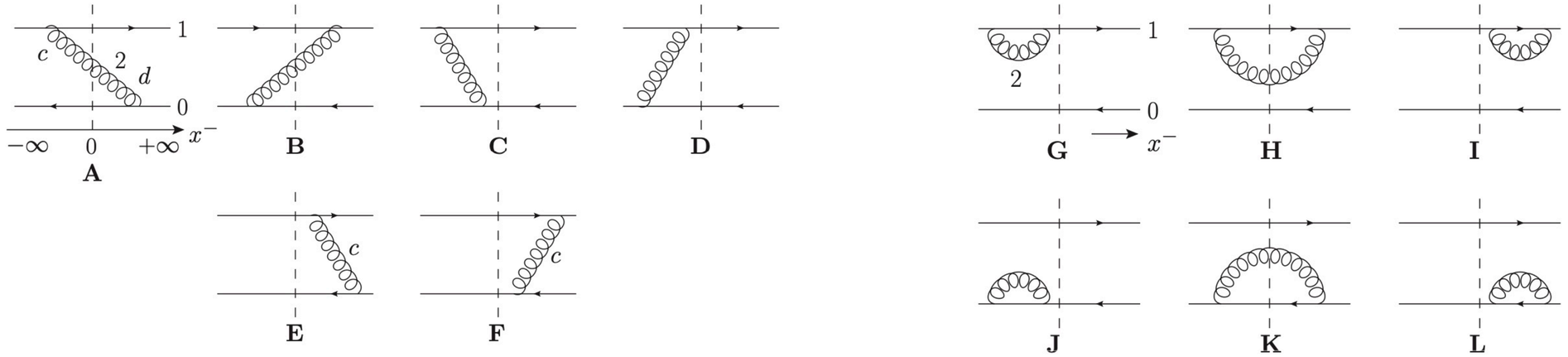

Balitsky hierarchy: an infinite set of evolution equations could be obtained; the evolution of n-Wilson line correlators can be derived from $(n+2)$-Wilson line correlators.

I. Balitsky, NPB463, 99-160 (1996)

$$\frac{\partial}{\partial Y}\langle S(x_{10})\rangle_Y = \frac{\alpha_s N_c}{2\pi^2}\int d^2x_2 \frac{x_{10}^2}{x_{20}^2 x_{21}^2}\left[\langle S(x_{12})S(x_{20})\rangle_Y - \langle S(x_{10})\rangle_Y\right]$$

$$\frac{\partial}{\partial Y}\langle S(x_{12})S(x_{20})\rangle_Y = \cdots$$

Not a closed-equation.
No analytic solutions.

Large-N_c limit and BK evolution

$$\langle S(x_{12})S(x_{20})\rangle_Y = \langle S(x_{12})\rangle_Y \langle S(x_{20})\rangle_Y + \mathcal{O}\left(\frac{1}{N_c}\right)$$

- Naive estimation of the $1/N_c$ corrections to BK equation: $1/N_c^2 \approx 11\,\%$
- However, the $1/N_c$ corrections are more suppressed due to the saturation effect.
- BK eq. can be a good approximation as long as IC. does not contain strong $1/N_c$ corrections

K. Rummukainen and H. Weigert, NPA739, 183-226 (2004)
Y. V. Kovchegov, J. Kuokkanen, K. Rummukainen and H. Weigert, NPA823, 47-82 (2009)

"nonplanner"

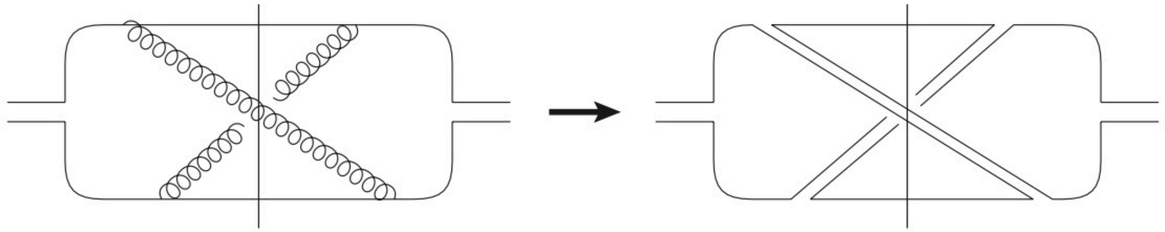

$$\sim \mathcal{O}\left(\frac{1}{N_c^2}\right)$$

"planner"

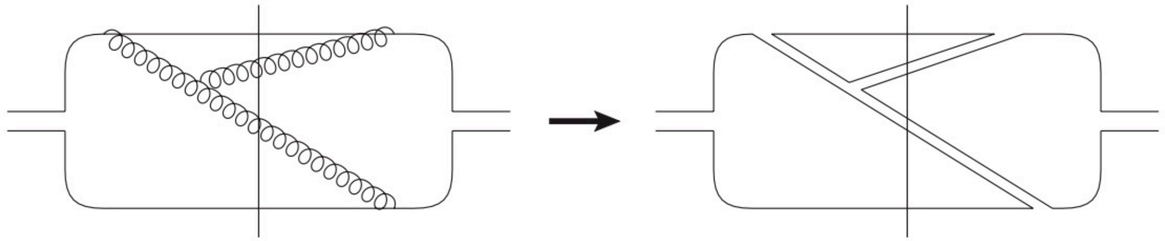

Balitsky-Kovchegov equation

I. Balitsky, NPB463 (1996),99

Y. Kovchegov, PRD60(1999), 034008

In terms of the dipole scattering amplitude $N = S - 1$:

$$\frac{\partial}{\partial Y} N(x_{10}, Y) = \frac{\alpha_s N_c}{2\pi^2} \int d^2x_2 \frac{x_{10}^2}{x_{20}^2 x_{21}^2} \left[N(x_{12}, Y) + N(x_{20}, Y) - N(x_{10}, Y) - N(x_{12}, Y) N(x_{20}, Y) \right]$$

Bremsstrahlung (BFKL) **Recombination**

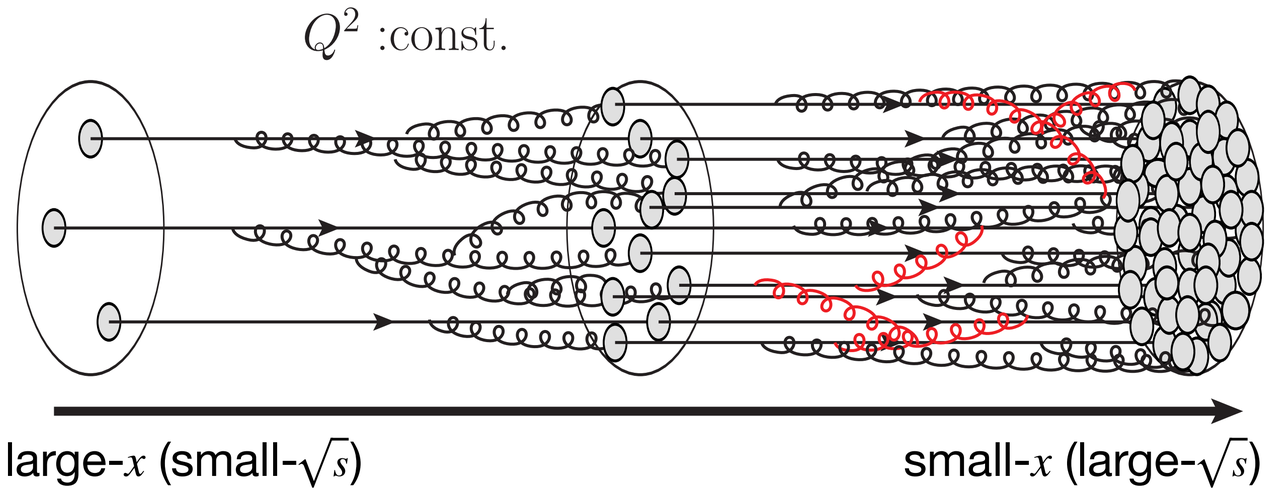

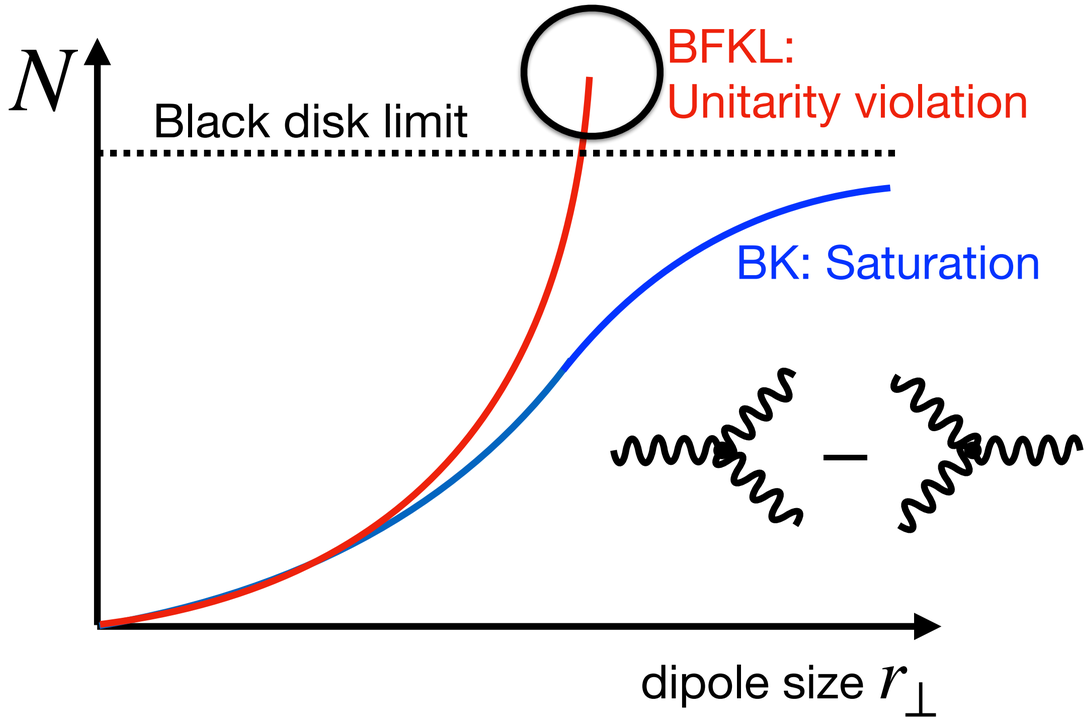

Nonlinear gluon fusion (two dipoles merging) slows down the quantum evolution speed and results in the saturation of the gluon density.

McLerran-Venugopalan model

L.McLerran and R. Venugopalan, Phys. Rev. D49 (1994) 2233; ibid. 49 (1994) 3352; ibid. 50 (1994) 2225

In a large nucleus, a probe of small-x does not resolve the longitudinal extent of the nucleus when $Q^2 \ll \Lambda^2_{\rm QCD} A^{1/3}$:

$$W_{Y_0}[\rho] = \exp\left[-\int d^2x_\perp \frac{\rho^a(x_\perp)\rho^a(x_\perp)}{2\mu_A^2(x_\perp)}\right]$$

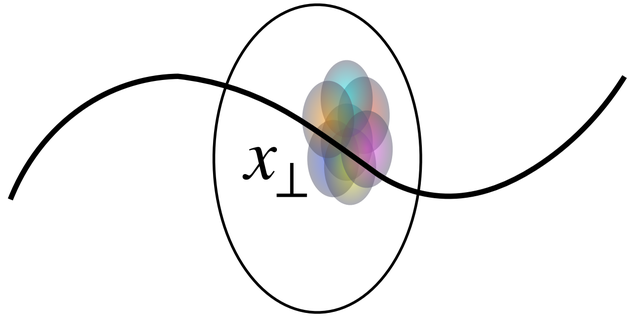

For $A \gg 1$, $\mu_A^2 \sim Q_{sA}^2 \propto A^{1/3} \gg \Lambda^2_{\rm QCD}$

Here we assume that $\langle\rho\rangle = 0$ and higher point functions vanish.

- **The main ides:** the color charge per unit area, $\rho(x_\perp)$, is the sum of the color charges of the partons that sit at approximately the same impact parameter $x_\perp$.
- Local correlations at $x_\perp$ as a consequence of confinement: color charges separated by more than the nucleon size cannot be correlated!

Rapidity evolution of the dipole amplitude

Parameters in the MV initial condition can be fitted by HERA inclusive data for $x \leq 0.01$.

$$\varphi_{p,Y}(k_\perp) = \pi R_p^2 \frac{N_c k_\perp^2}{4\alpha_s} \mathcal{N}_Y^A(k_\perp)$$

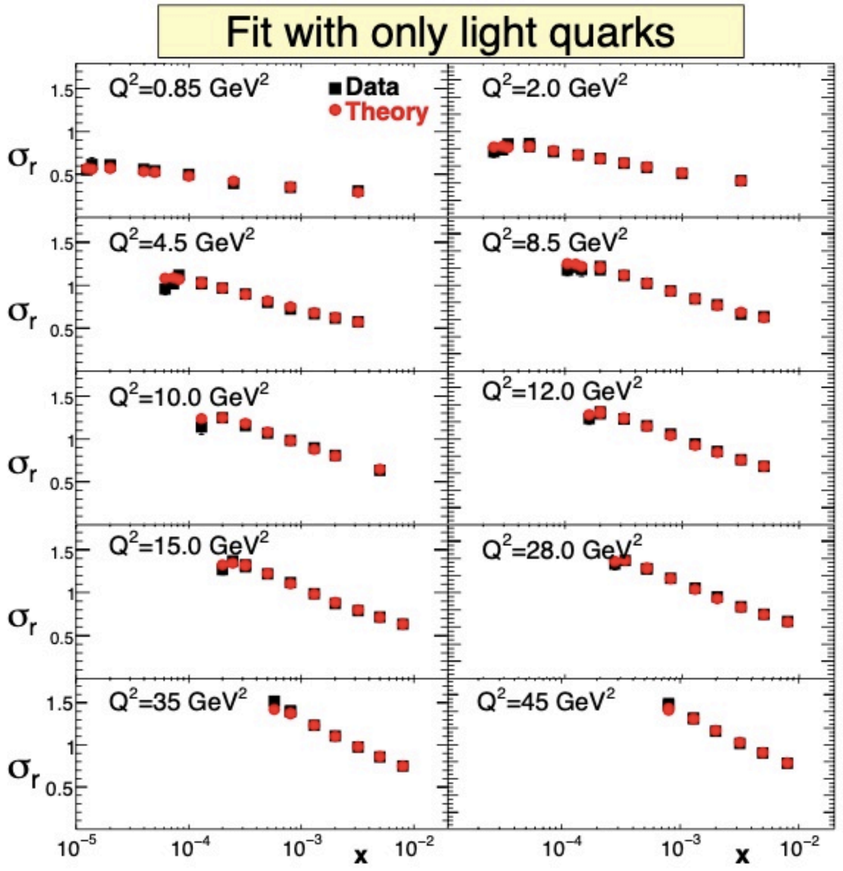

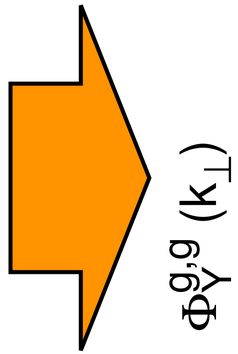

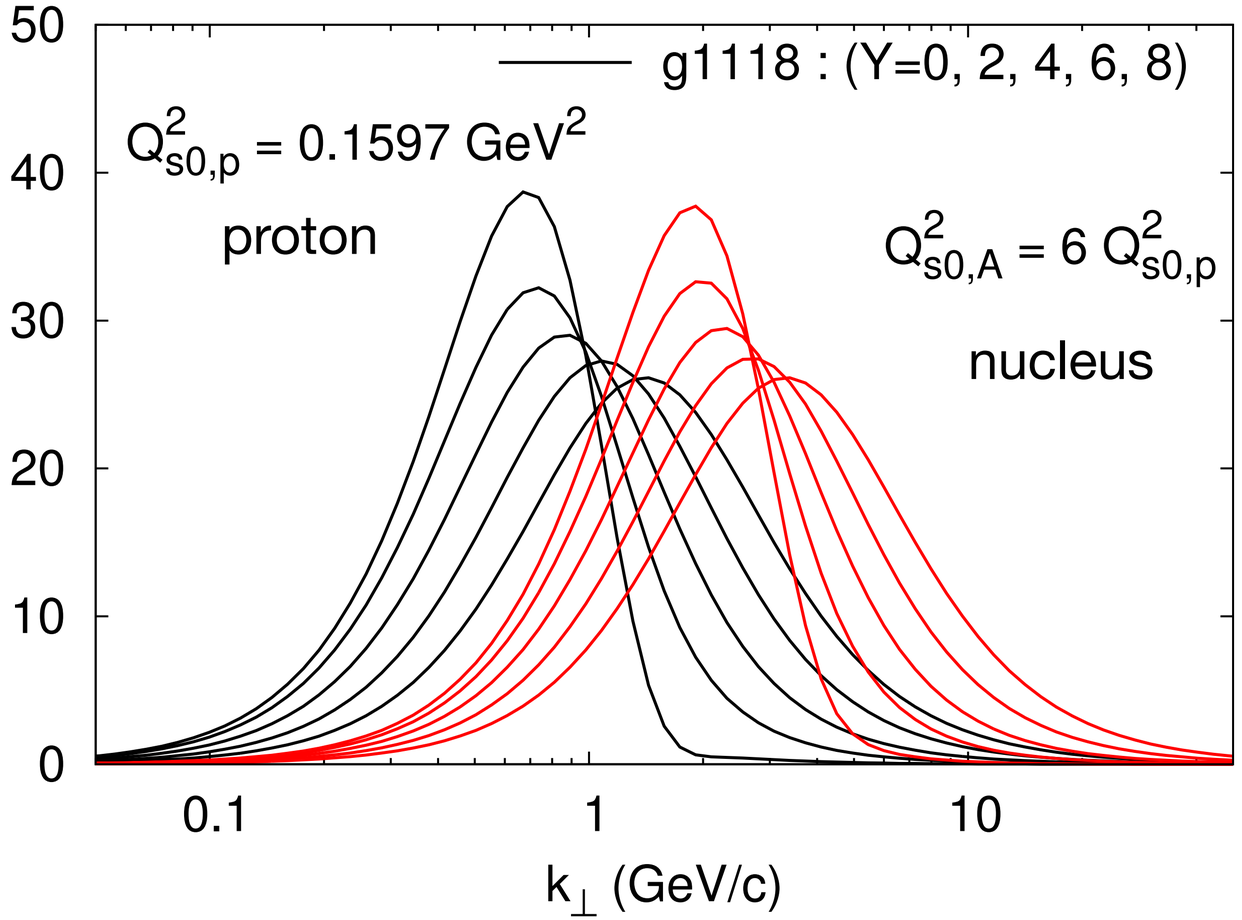

The rapidity dependence of Q_s^2

Solving rcBK equation

$$\mathcal{N}_Y(r_\perp = 1/Q_s) = 0.5$$

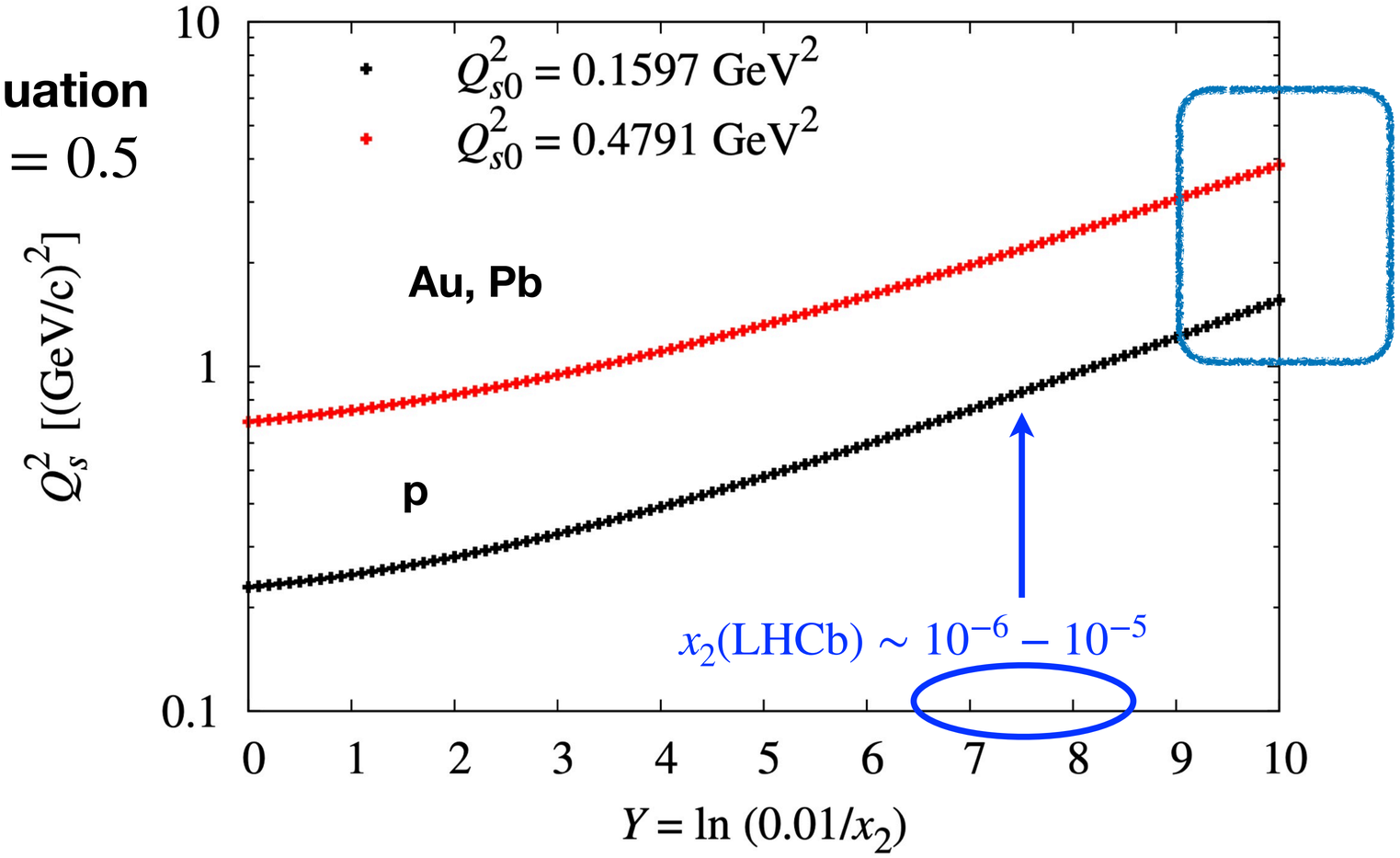

the same slope asymptotically

❖ If nuclear target is saturated, it could behave like a "big" proton.

Remarks on Scaling

❖ BK equation reduces to Fisher and Kolmogorov-Petrovsky-Piscounov (FKPP) equation, whose dynamics is reaction-diffusion dynamics, only when k_t is in the vicinity of the saturation scale:

$$\partial_t u(x,t) = \partial_x^2 u(x,t) + u(x,t)(1 - u(x,t))$$

❖ FKPP equation allows traveling wave solutions; At larger times (t), the shape of a traveling wave is preserved.

In saturation physics, the position of the wavefront is nothing but the saturation scale. Geometric scaling may be interpreted as the traveling wave properties of the solution to the BK equation.

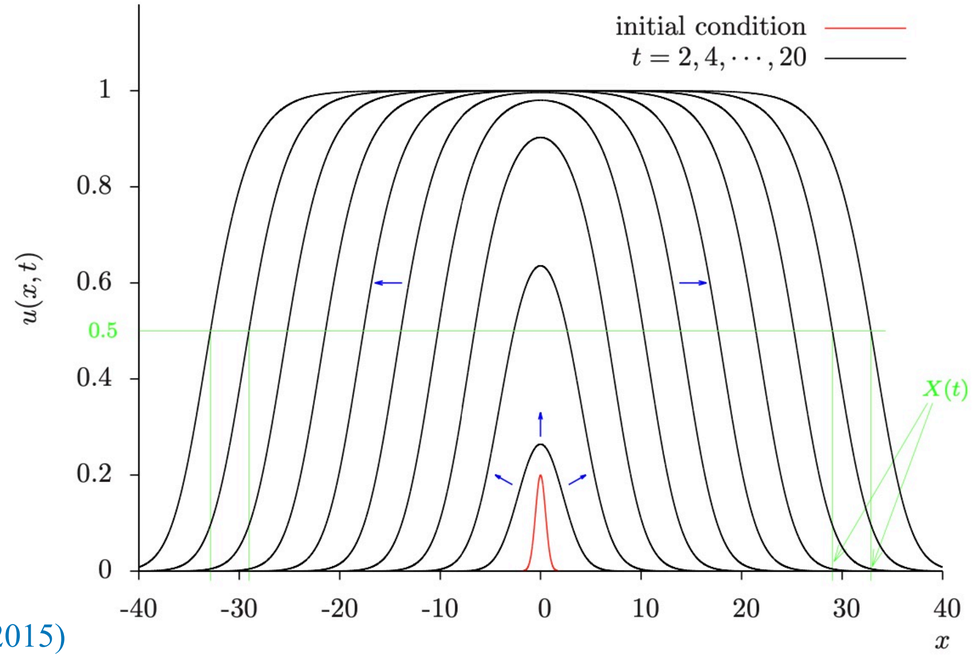

S. Munier, Sci. China Phys. Mech. Astron. 58, no.8, 81001 (2015)

Part II:

Phenomenology and some features on saturation effects

1. Inclusive particle production
2. TMDs and CGC at small-x

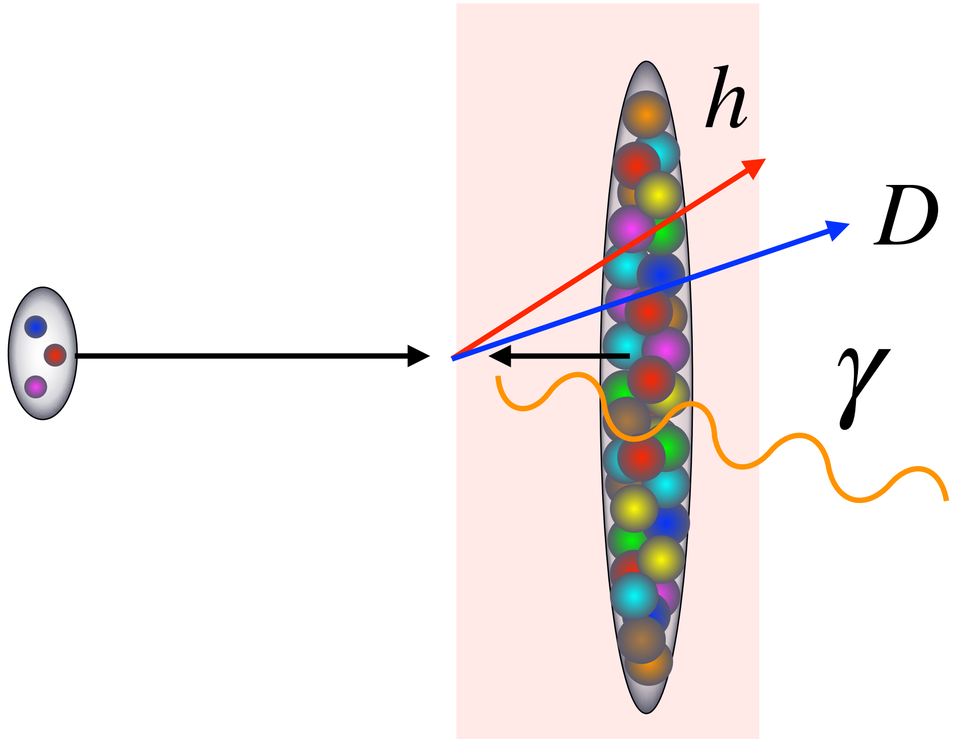

Kinematics to be considered

(i) Mid rapidity region:

- $x_1 \sim x_2 < 1$

(ii) Forward rapidity region:

- $x_1 \sim \mathcal{O}(1),\ x_2 \ll 1$

(iii) Backward rapidity region:

- $x_2 \sim \mathcal{O}(1),\ x_1 \ll 1$

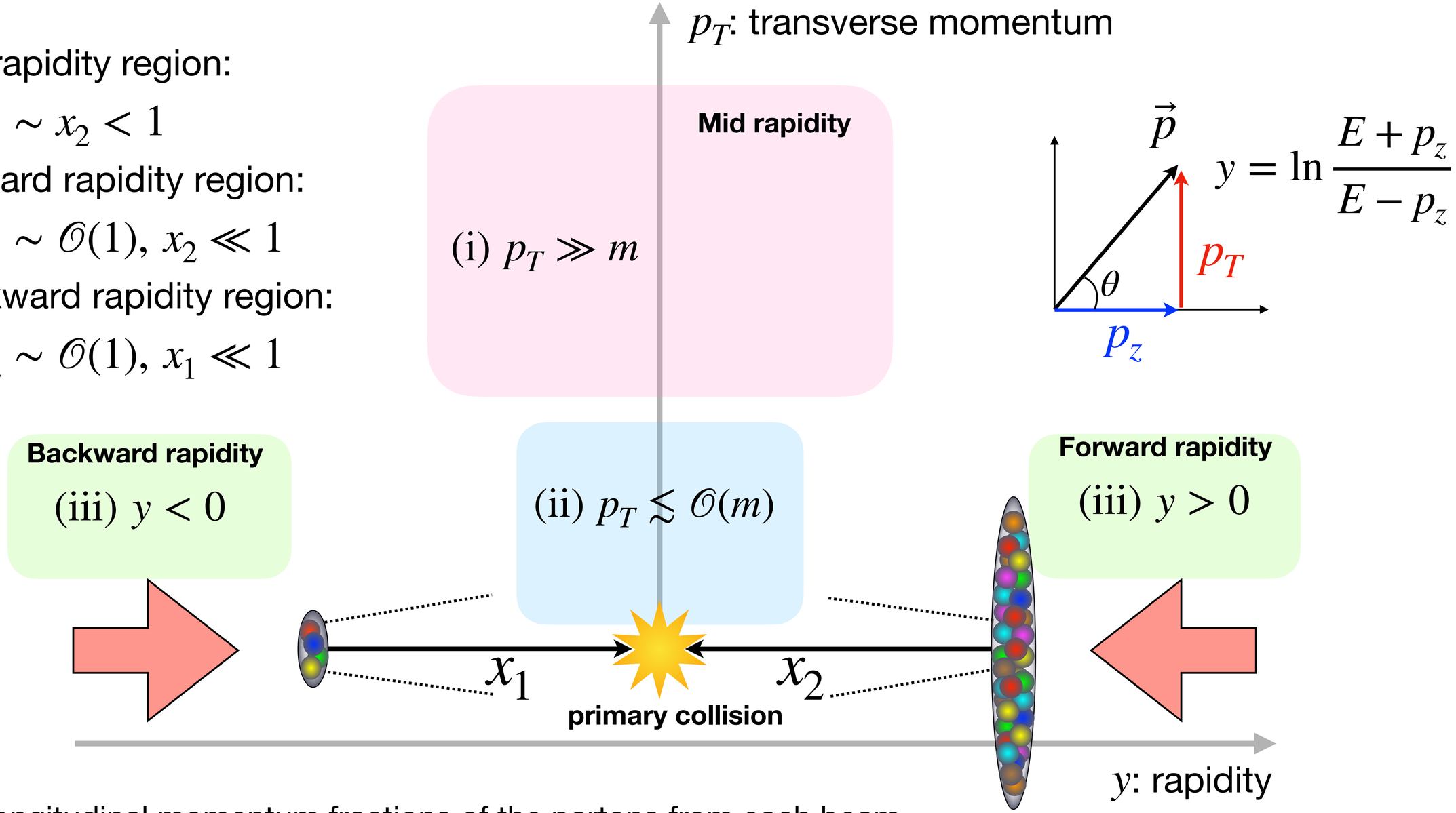

$x_{1,2}$: the longitudinal momentum fractions of the partons from each beam.

Inclusive particle production in hadronic collisions

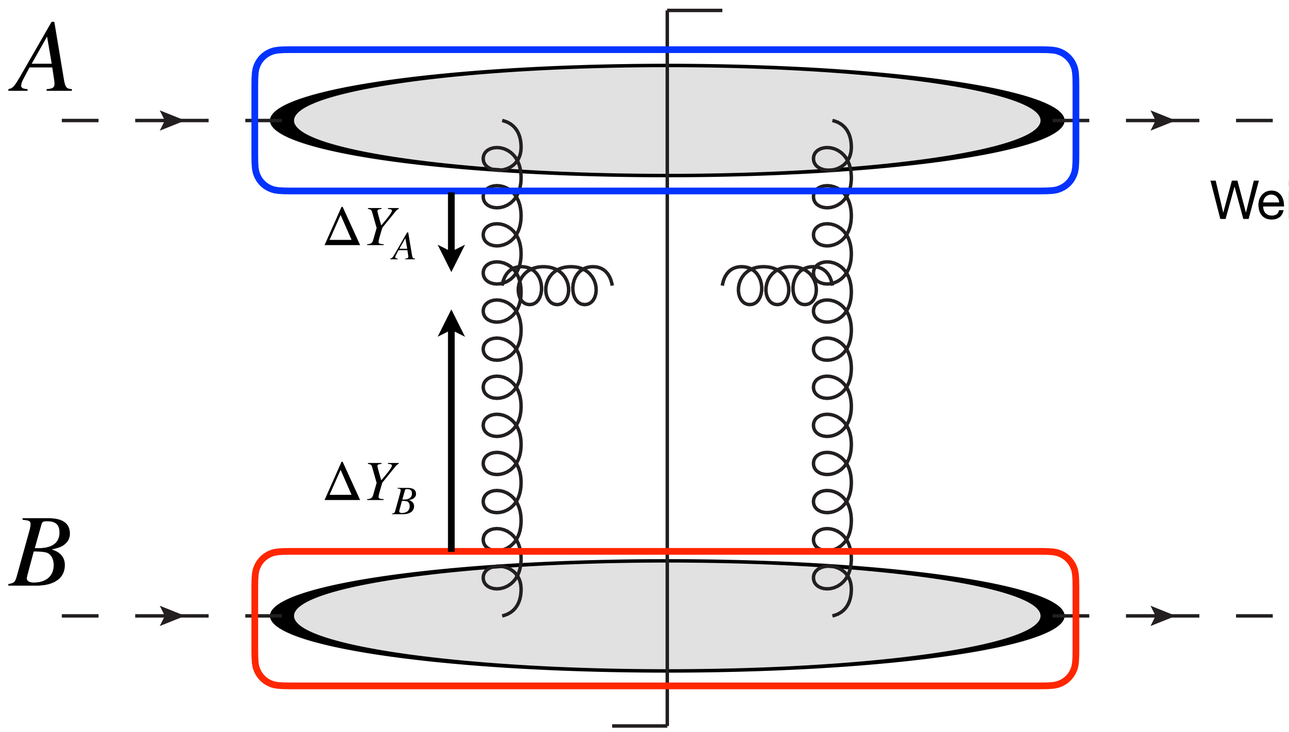

Weight functionals are universal.

$$J^\nu = \delta^{+\nu}\rho_A + \delta^{-\nu}\rho_B$$

pp vs. pA vs. AA
→ different combinations of Q_A^2 and Q_B^2

$$\langle \mathcal{O} \rangle = \int [\mathcal{D}\rho_A] W_{Y_A}[\rho_A] [\mathcal{D}\rho_B] W_{Y_B}[\rho_B] \mathcal{O}[\rho_A, \rho_B]$$

- If $\Delta Y_A \ll \Delta Y_B$ such as particle production in pp/pA at forward rapidity, $Q_{s,A}^2 \ll Q_{s,B}^2$
- Hybrid factorization ansatz: collinear factorization with PDFs describes projectile.

Charged hadron multiplicity in pA collisions

A. Dumitru, D. E. Kharzeev, E. M. Levin and Y. Nara, PRC85, 044920 (2012)

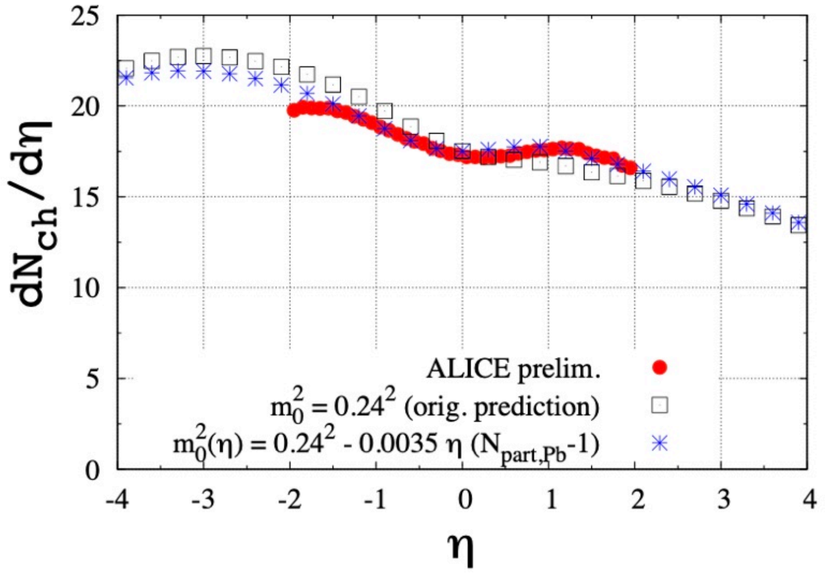

KLN saturation model

J. L. Albacete, A. Dumitru, H. Fujii and Y. Nara, NPA897, 1-27 (2013)

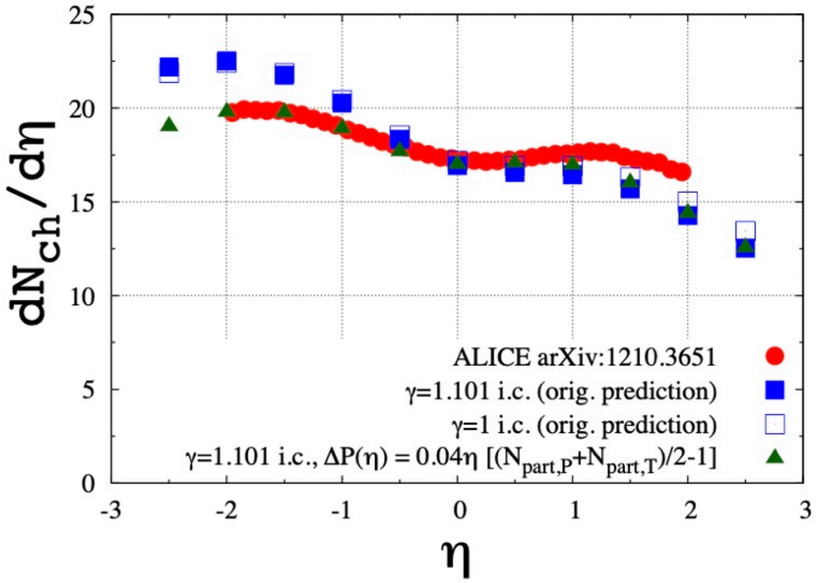

rcBK equation

P. Tribedy and R. Venugopalan, PLB710, 125-133 (2012) [erratum: PLB718, 1154-1154 (2013)]

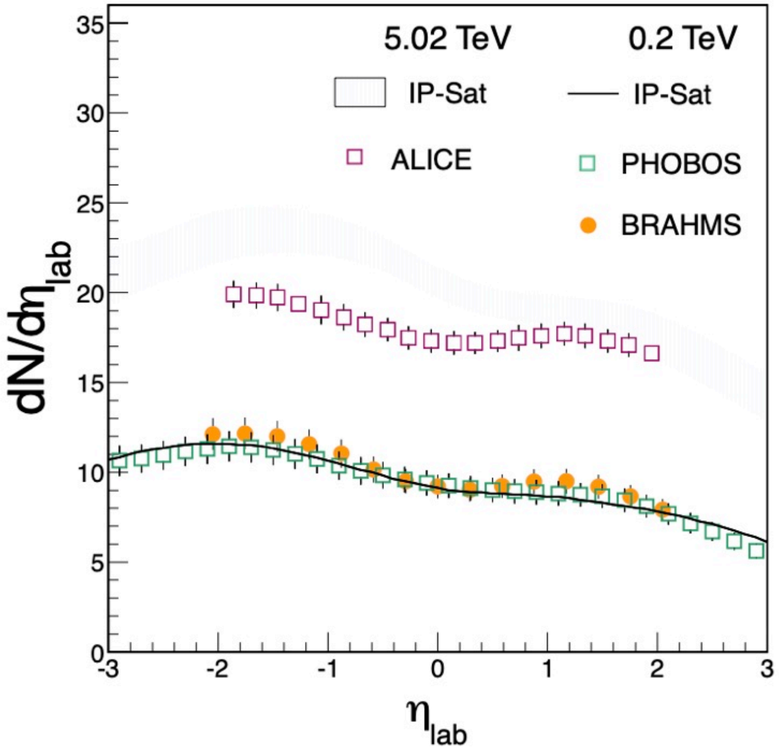

IP-Sat

Hybrid factorization for a dilute-dense system

$$\frac{d\sigma_{p+A\to h+X}}{dyd^2p_T} = \int x_p f_{a/p}(x_p) \otimes \mathscr{F}_a(k_\perp) \otimes D_a^h(z) \otimes \mathscr{H}^{(0)}$$

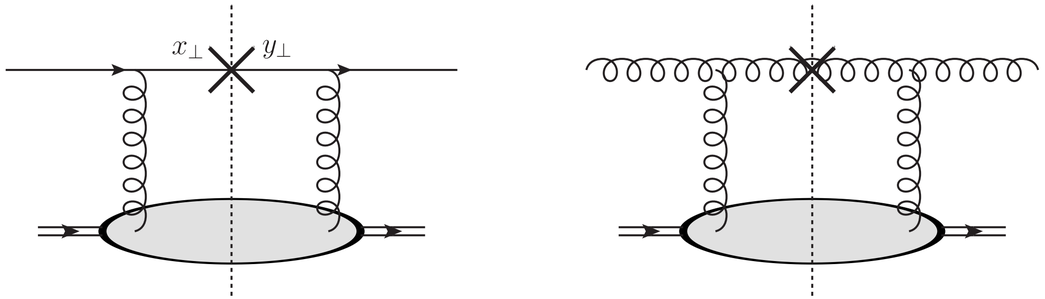

- Dilute projectile: collinear PDFs
- Dense target: Wilson line correlators $\mathscr{F}$ (not standard parton densities)
- Room for NLO corrections

A. Dumitru, A. Hayashigaki and J. Jalilian-Marian, NPA765, 464-482 (2006)

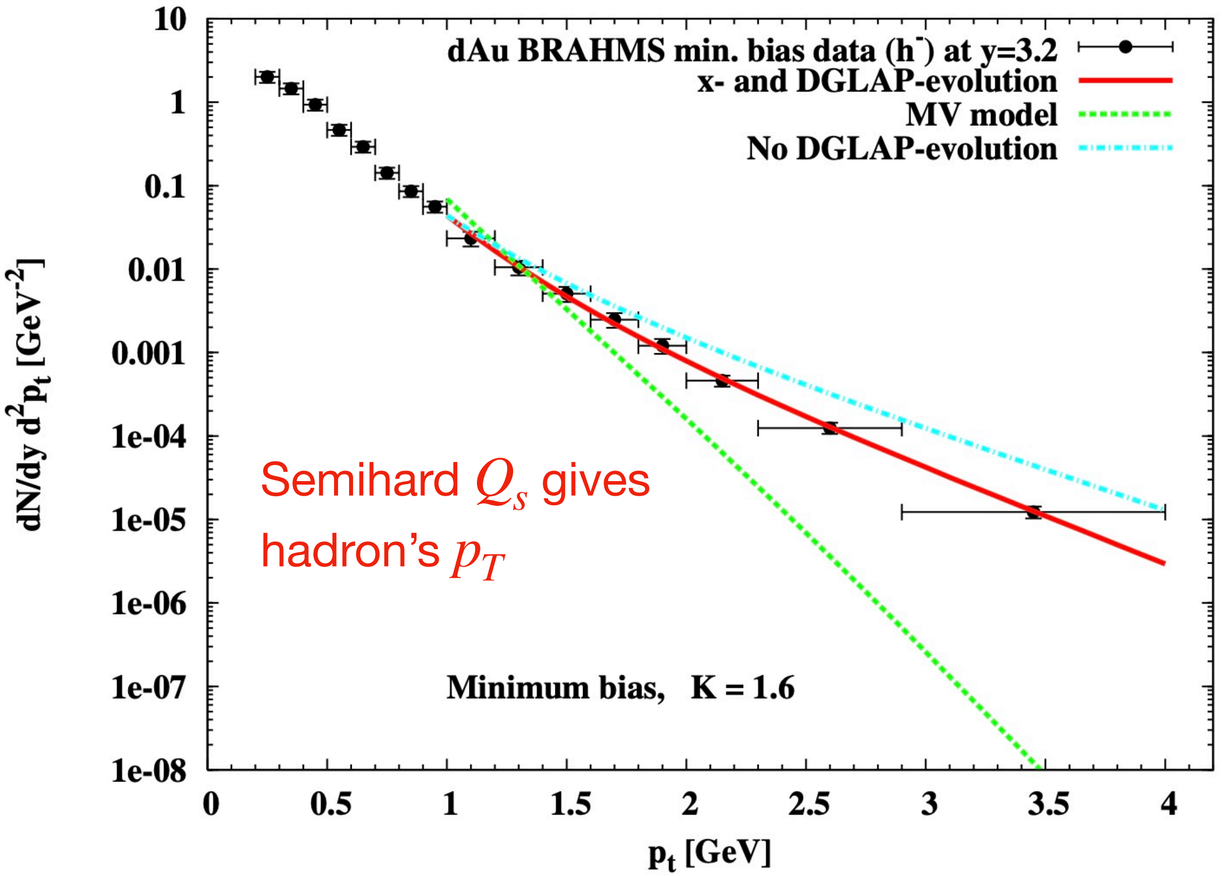

NLO corrections

$$\frac{d\sigma_{p+A\to h+X}}{dyd^2p_T} = \int x_p f_{a/p}(x_p) \otimes \mathscr{F}_a(k_\perp) \otimes D_a^h(z) \otimes \mathscr{H}^{(0)}$$

$$+\frac{\alpha_s}{2\pi}\int xf_{a/p}(x) \otimes \mathscr{F}_{ab}(k_\perp) \otimes D_b^h(z) \otimes \mathscr{H}^{(1)}$$

Real

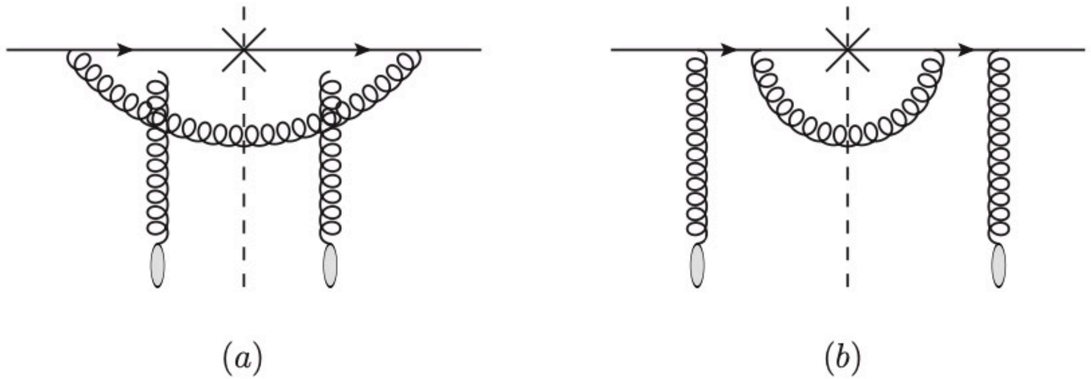

Virtual

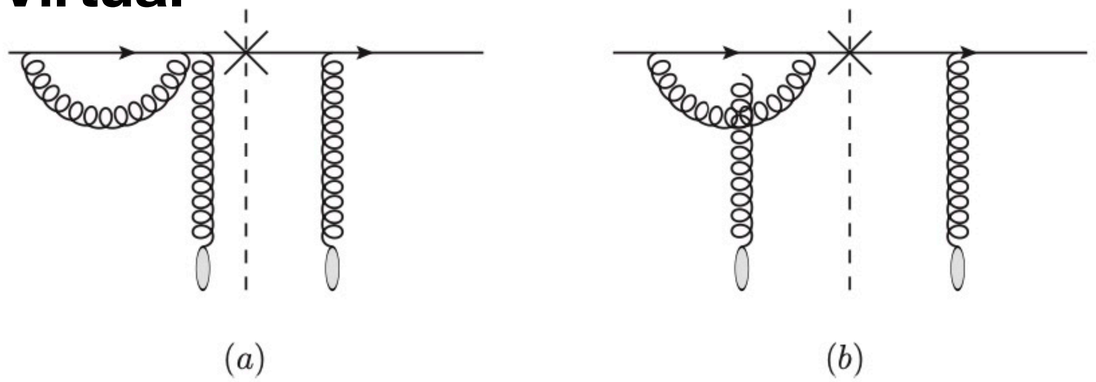

Relevant channels:

$qg \to qg, \quad gg \to gg, \quad gg \to q\bar{q}$

Master equations at NLO

G. A. Chirilli, B.W. Xiao and F. Yuan, PRD86, 054005 (2012)

$$\frac{d\sigma^{p+A\to h+X}}{d^2p_{h\perp}dy}=\sum_f\int_\tau^1\frac{dz}{z^2}\int_{x_p}^1\frac{dx}{x}\xi\left(xq_f\left(x,\mu\right),xG\left(x,\mu\right)\right)\begin{pmatrix}S_{qq}^{(0)}+\frac{\alpha_s}{2\pi}S_{qq} & \frac{\alpha_s}{2\pi}S_{gq}\\ \frac{\alpha_s}{2\pi}S_{qg} & S_{gg}^{(0)}+\frac{\alpha_s}{2\pi}S_{gg}\end{pmatrix}\begin{pmatrix}D_{h/q}(z,\mu)\\ D_{h/g}(z,\mu)\end{pmatrix}$$

$$\begin{pmatrix}q_f(x,\mu)\\ G(x,\mu)\end{pmatrix}=\begin{pmatrix}q_f^{(0)}(x)\\ G^{(0)}(x)\end{pmatrix}-\frac{1}{\hat\epsilon}\frac{\alpha_s(\mu)}{2\pi}\int_z^1\frac{d\xi}{\xi}\begin{pmatrix}C_F\mathscr{P}_{qq}(\xi)T_R\mathscr{P}_{qg}(\xi)\\ \sum_f C_F\mathscr{P}_{gq}(\xi)N_c\mathscr{P}_{gg}(\xi)\end{pmatrix}\begin{pmatrix}q_f(x/\xi)\\ G(x/\xi)\end{pmatrix}$$

$$\begin{pmatrix}D_{h/q}(z,\mu)\\ D_{h/g}(z,\mu)\end{pmatrix}=\begin{pmatrix}D_{h/q}^{(0)}(z)\\ D_{h/g}^{(0)}(z)\end{pmatrix}-\frac{1}{\hat\epsilon}\frac{\alpha_s(\mu)}{2\pi}\int_z^1\frac{d\xi}{\xi}\begin{pmatrix}C_F\mathscr{P}_{qq}(\xi)C_F\mathscr{P}_{gq}(\xi)\\ \sum_f T_R\mathscr{P}_{qg}(\xi)N_c\mathscr{P}_{gg}(\xi)\end{pmatrix}\begin{pmatrix}D_{h/q}(z/\xi)\\ D_{h/g}(z/\xi)\end{pmatrix}$$

$$\mathscr{F}(k_\perp)=\mathscr{F}^{(0)}(k_\perp)-\frac{\alpha_sN_c}{2\pi^2}\int_0^1\frac{d\xi}{1-\xi}\int\frac{d^2x_\perp d^2y_\perp d^2b_\perp}{(2\pi)^2}e^{-ik_\perp\cdot(x_\perp-y_\perp)}\frac{(x_\perp-y_\perp)^2}{(x_\perp-b_\perp)^2(y_\perp-b_\perp)^2}\left[S_Y^{(2)(x_\perp,y_\perp)}-S_Y^{(4)(x_\perp,b_\perp,y_\perp)}\right]$$

- ❖ Colliner divergences → PDFs and FFs.
- ❖ Rapidity divergence → Wilson line correlators.

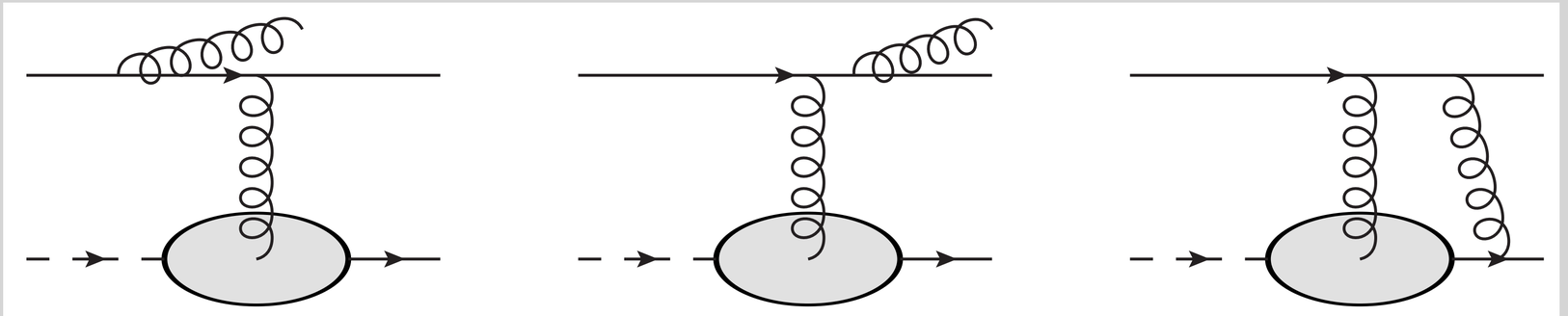

First numerical computations: LO + NLO

A. M. Stasto, B. W. Xiao and D. Zaslavsky, PRL112, no.1, 012302 (2014)

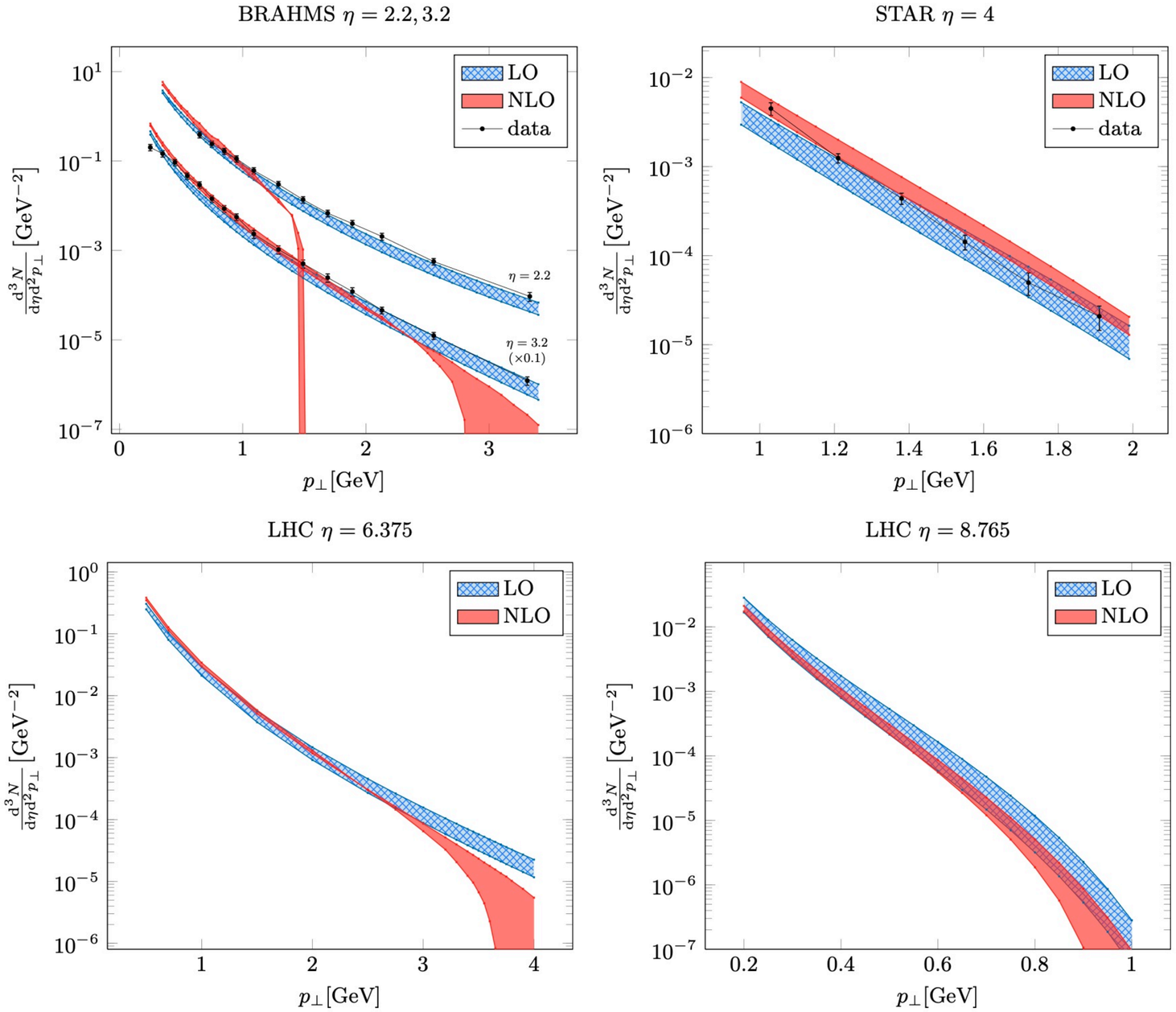

Toward the precision era

KW, Xiao, Yuan and Zaslavsky, PRD92, no.3, 034026 (2015)

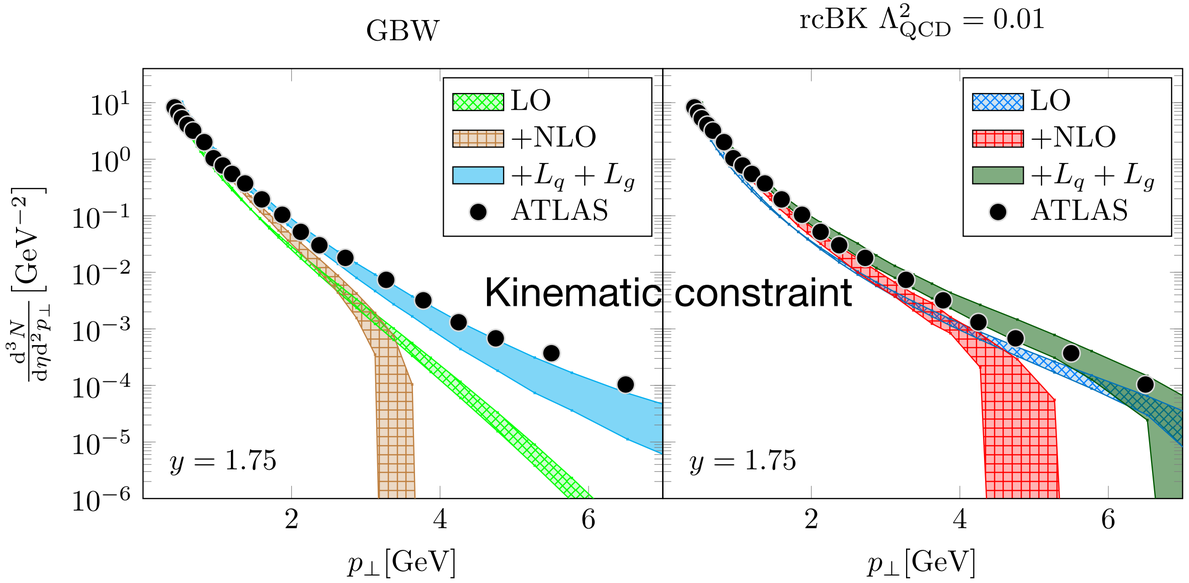

Y. Shi, L. Wang, S.Y. Wei and B.W. Xiao, PRL128, no.20, 202302 (2022)

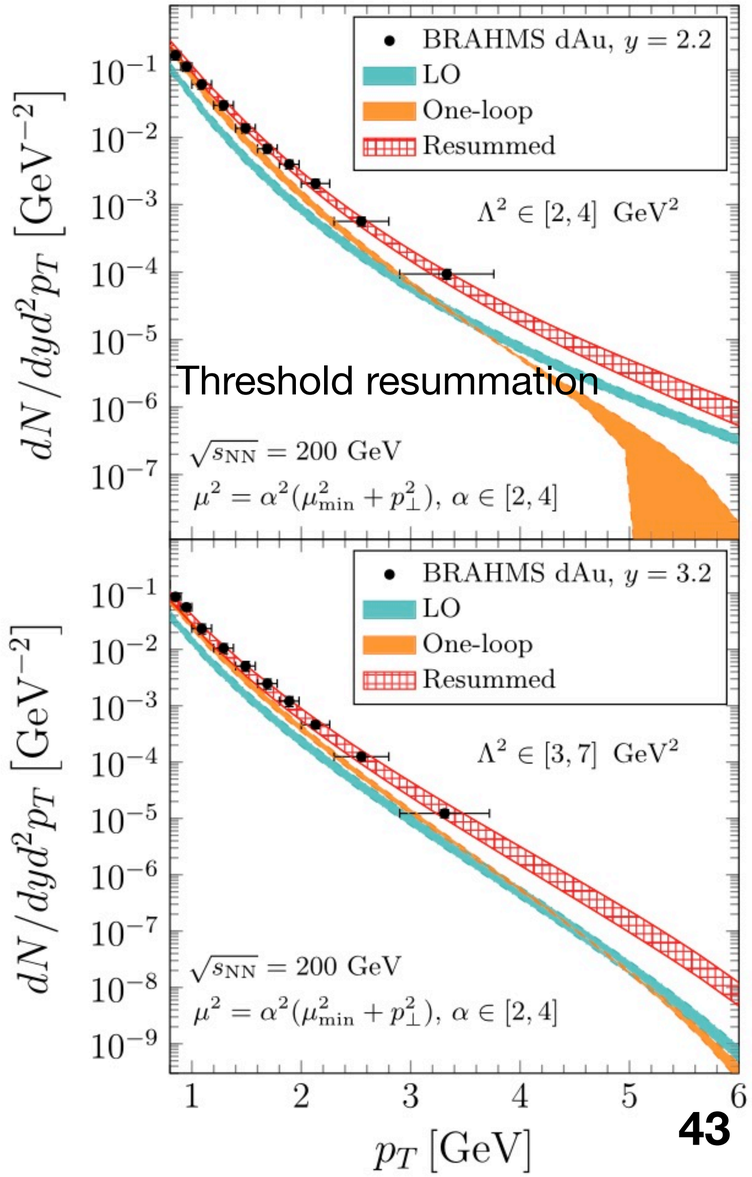

Liu, Ma and Chao, PRD100, no.7, 071503 (2019)

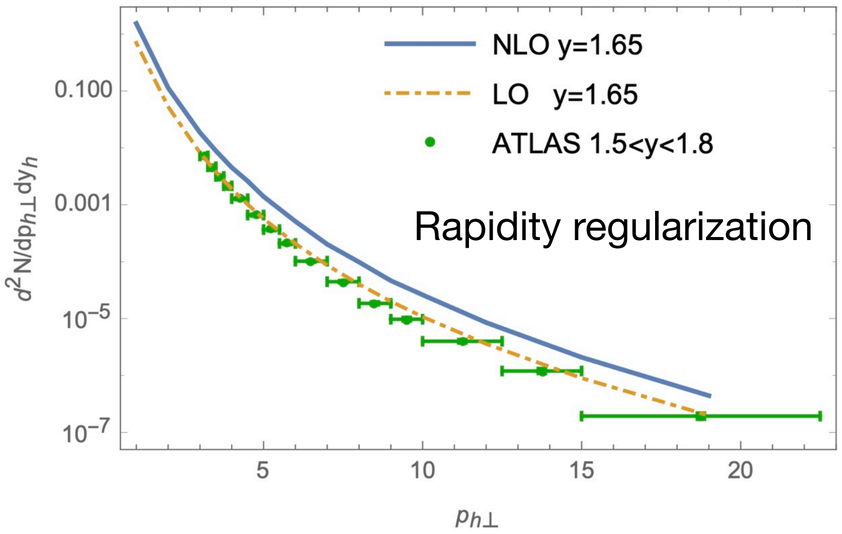

Liu, Kang and Liu, PRD102, no.5, 051502 (2020)

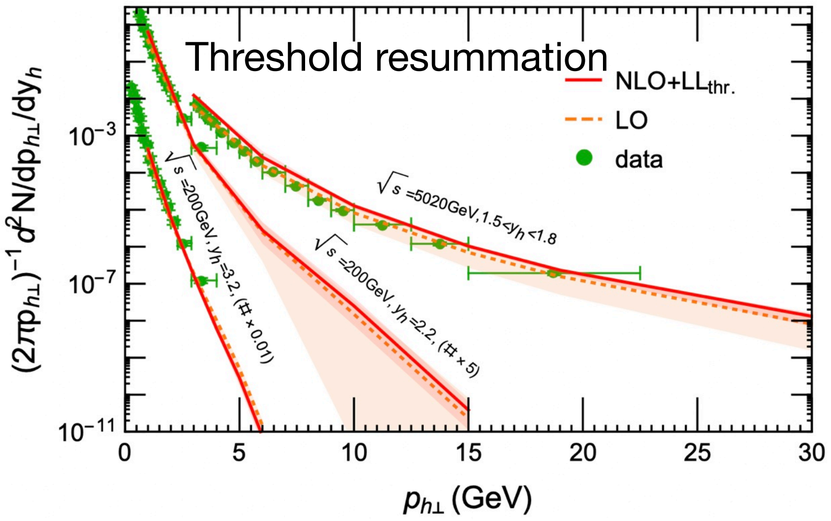

Dijet production in DIS at NLO: cutting-edge

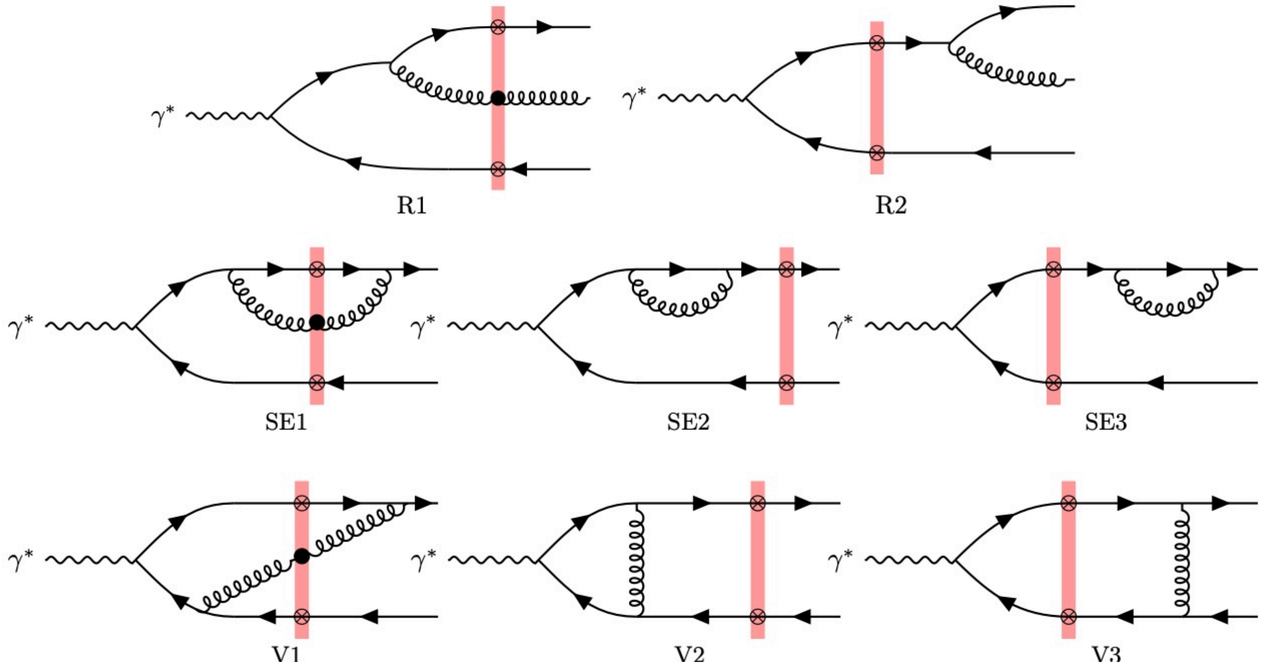

To define jets, k_t algorithm, anti-k_t algorithm, and the Cambridge/Aachen algorithm are applicable. → NLO hard factors.

P. Caucal, F. Salazar, B. Schenke, T. Stebel and R. Venugopalan, JHEP08, 062 (2023)

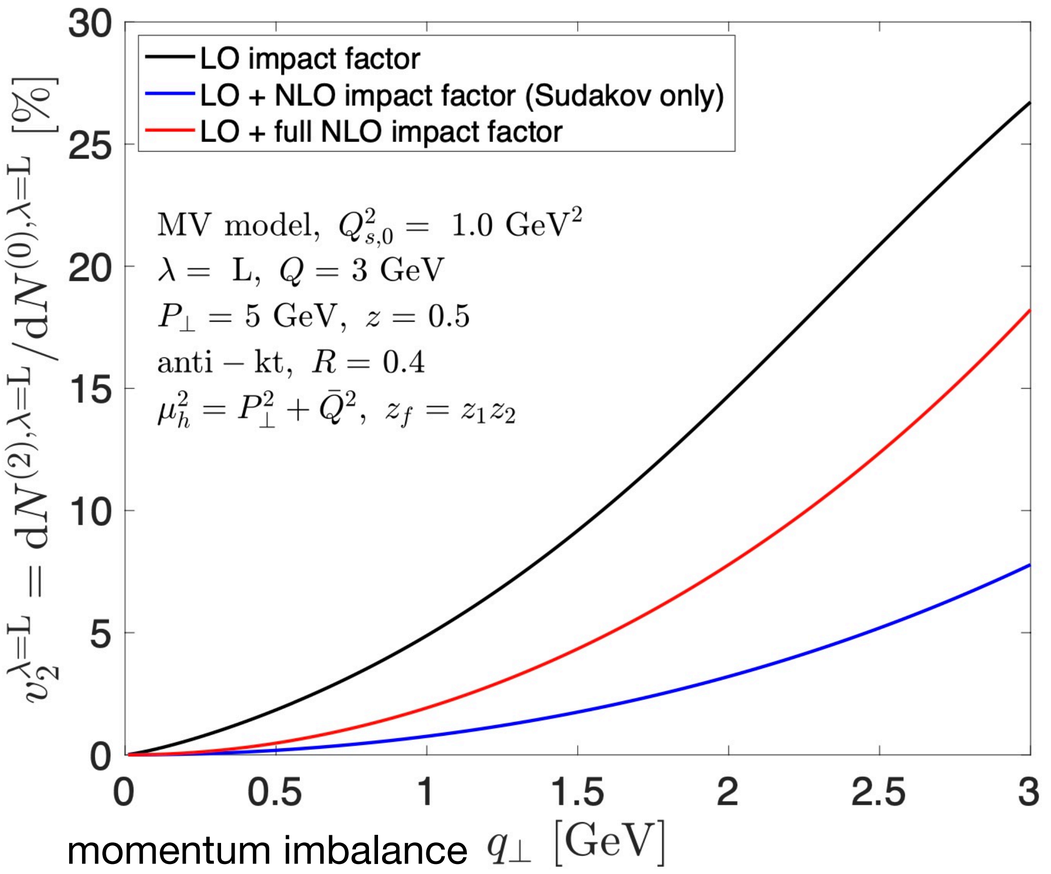

Two distinct approaches

❖ TMD approach

✓ TMD factorization is valid for all x.

✓ Leading twist (+ subleading power)

✓ On-shell hard scattering parts with transverse-momentum-dependent PDFs.

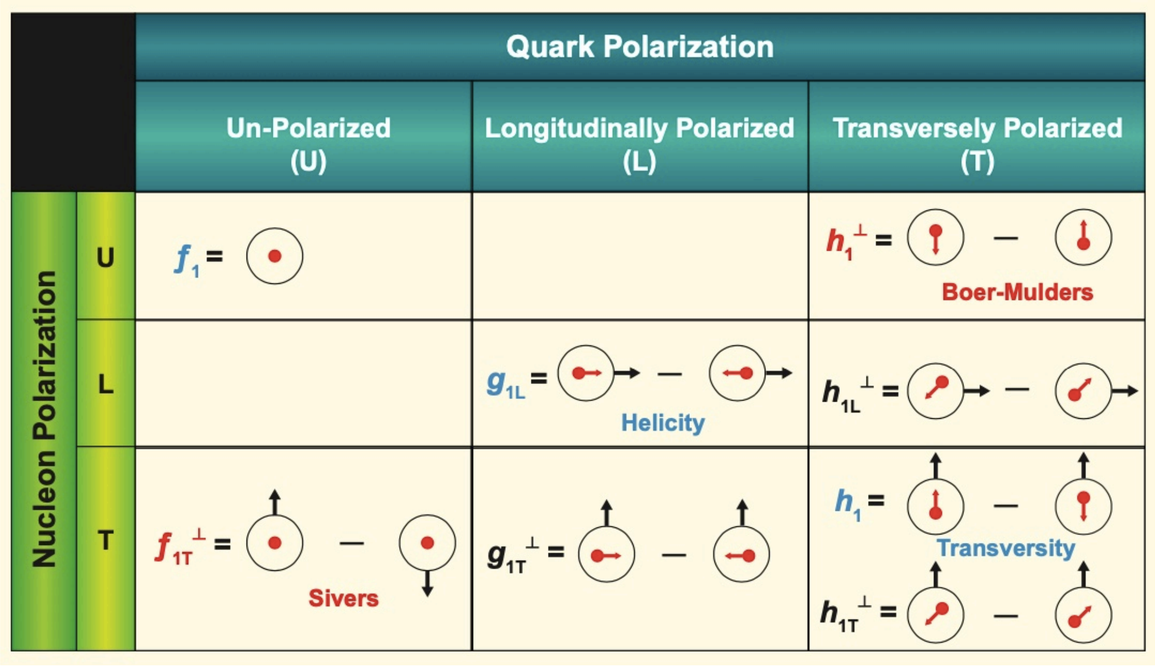

❖ CGC approach

✓ Only valid at $x \ll 1$.

✓ Higher twist contributions are included.

✓ Off-shellness of hard parts is taken into account.

✓ Multi-point Wilson line correlators

NAS report

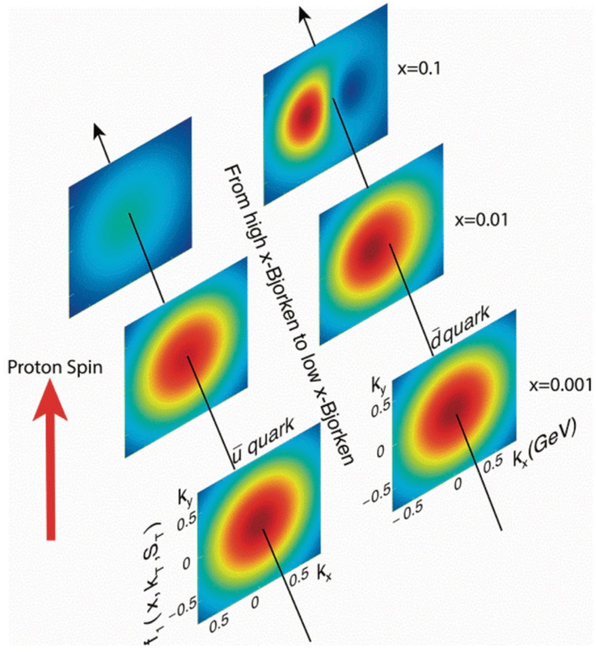

Process dependent gluon distributions

F. Dominguez, C. Marquet, B.-W. Xiao and F. Yuan, PRD83, 105005 (2011)

	DIS and DY	SIDIS	hadron in pA	photon-jet in pA	Dijet in DIS	Dijet in pA
$G^{(1)}$ (WW)	×	×	×	×	√	√
$G^{(2)}$ (dipole)	√	√	√	√	×	√

Weizsäcker-Williams gluon distribution function (Number density of gluon)

$$xG^{(1)}(x,k_\perp) = \int \frac{2d\xi^- d^2\xi_\perp}{(2\pi)^3 P^+} e^{ixP^+\xi^- - ik_\perp\cdot\xi_\perp} \left\langle P \left| \mathrm{Tr}\left[F^{+i}(\xi^-,\xi_\perp)\mathcal{U}^{[+]\dagger}F^{+i}(0)\mathcal{U}^{[+]}\right] \right| P \right\rangle$$

Unintegrated dipole gluon distribution function (Not clear partonic picture)

$$xG^{(2)}(x,k_\perp) = \int \frac{2d\xi^- d^2\xi_\perp}{(2\pi)^3 P^+} e^{ixP^+\xi^- - ik_\perp\cdot\xi_\perp} \left\langle P \left| \mathrm{Tr}\left[F^{+i}(\xi^-,\xi_\perp)\mathcal{U}^{[-]\dagger}F^{+i}(0)\mathcal{U}^{[+]}\right] \right| P \right\rangle$$

Process dependent gauge links:

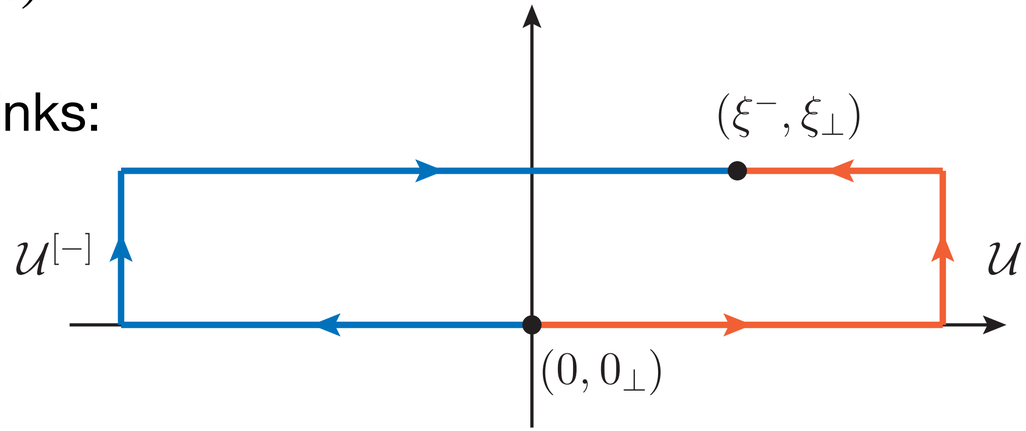

IS interactions

FS interactions

Universality at small-x

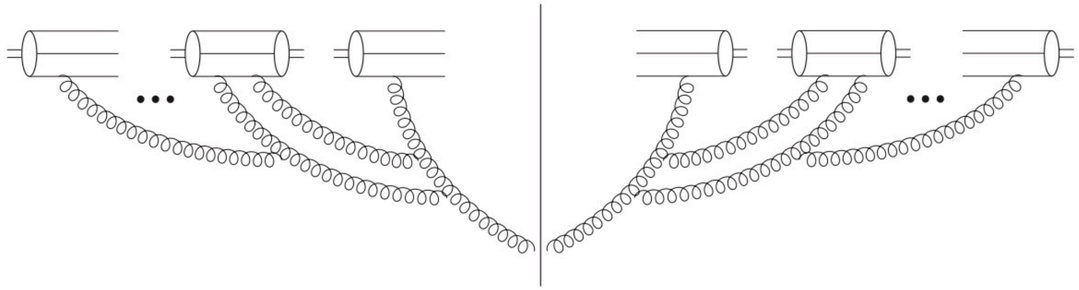

WW distribution can be evaluated using MV model at small-x and for a large nucleus only when a Gaussian distribution of ρ is used.

$$xG^{(1)}(x,k_\perp) \simeq \frac{2C_F S_\perp}{\pi^2 \alpha_s} \int \frac{d^2 r_\perp}{(2\pi)^2} \frac{e^{-ik_\perp \cdot r_\perp}}{r_\perp^2} \left[1 - e^{-\frac{1}{4} r_\perp^2 Q_s^2}\right]$$

Dipole distribution can be naturally related to the colo-dipole cross-section in CGC:

$$xG^{(2)}(x,k_\perp) \simeq \frac{N_c S_\perp k_\perp^2}{2\pi^2 \alpha_s} \int \frac{d^2 r_\perp}{(2\pi)^2} \frac{e^{-ik_\perp \cdot r_\perp}}{r_\perp^2} \frac{1}{N_c} \langle \mathrm{Tr}\left[U(0) U^\dagger(r_\perp)\right] \rangle$$

Things get more complicated when considering processes involving more gluons.

From TMD to CGC

k_t : off-shellness in short distance parts

Q : a hard scale.

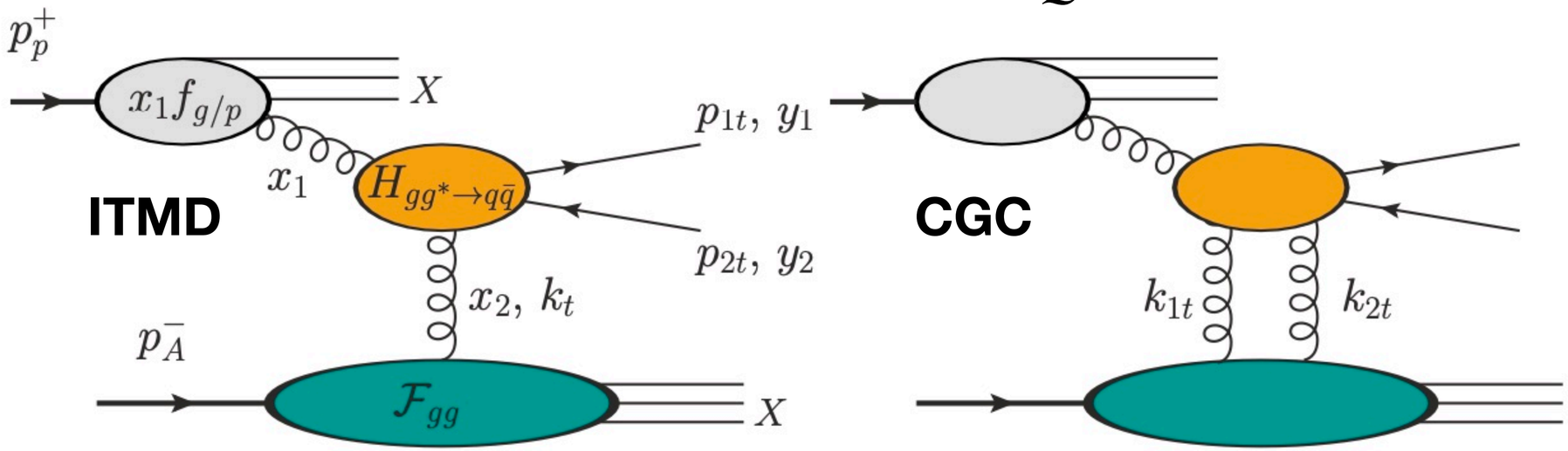

Altinoluk, Boussarie and Kotko, JHEP05, 156 (2019).
Mantysaari, Mueller, Salazar and Schenke, PRL124, no.11, 112301 (2020).
Fujii, Marquet and **KW**, JHEP12, 181 (2020).
Altinoluk, Marquet and Taels, JHEP06, 085 (2021).
Boussarie, Mantysaari, Salazar and Schenke, [arXiv:2106.11301 [hep-ph]].
…

- σ_{TMD} + kinematic twist $\mathcal{O}\left(\frac{k_t}{Q}\right)$ = Improved TMD (ITMD)
- σ_{ITMD} + higher-body genuine twist $\mathcal{O}\left(\frac{Q_s}{Q}\right)$ = CGC

Twist effects in forward dijet production

H. Fujii, C. Marquet and **KW**, JHEP12, 181 (2020)

LHC

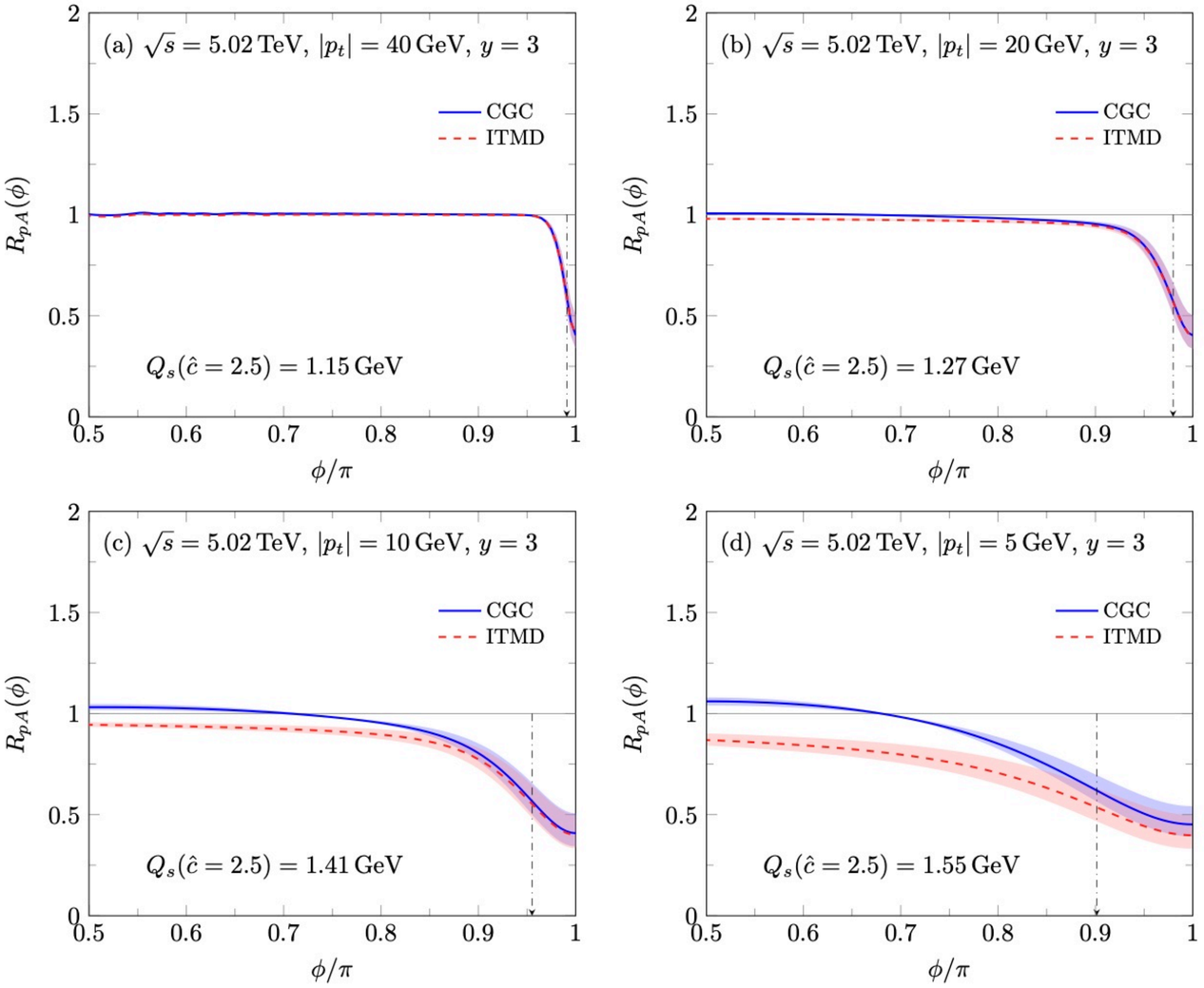

RHIC

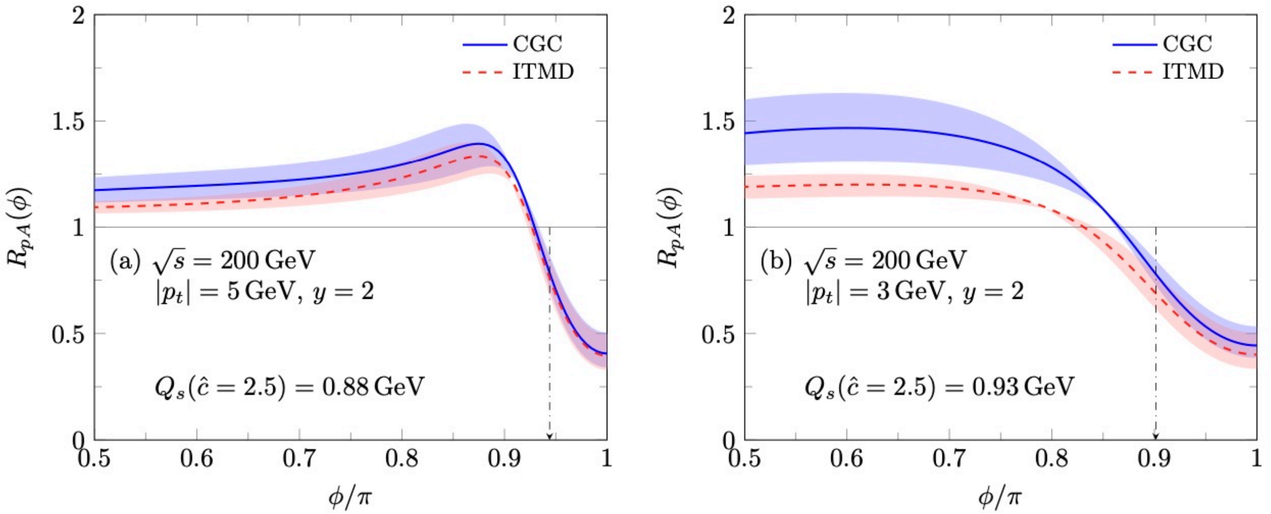

Dijet correlation is a good playground for studying the twist effects.

- Near-side: large intrinsic k_t
- Away-side: large genuine-twist

From CGC to Glasma and …

T. Lappi and L. McLerran, NPA772, 200-212 (2006)

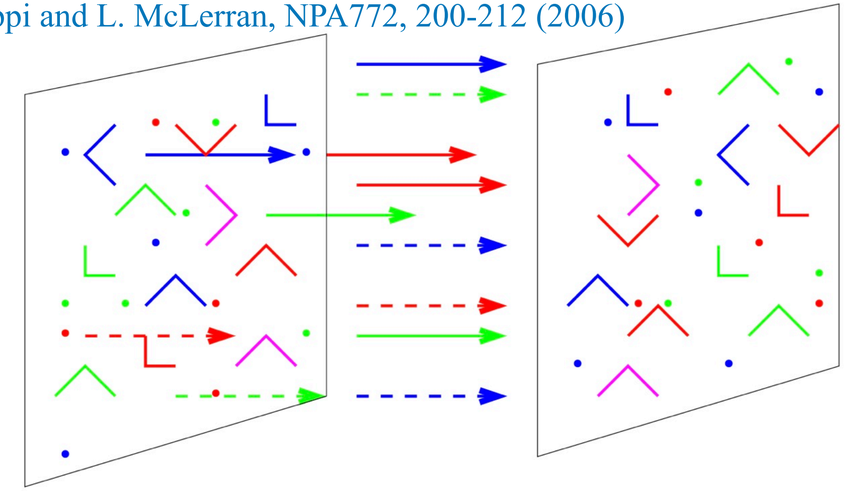

A. Ipp, D. I. Muller and D. Schuh, PLB810, 135810 (2020)

Jet momentum broadening

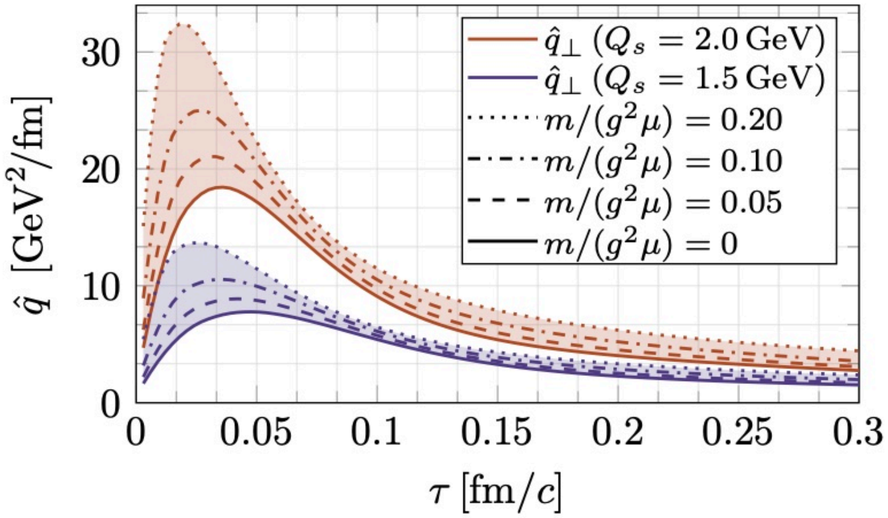

D. Avramescu, V. Baran, V. Greco, A. Ipp, D. I. Muller and M. Ruggieri, PRD107, no.11, 114021 (2023)

Heavy quarks trajectory

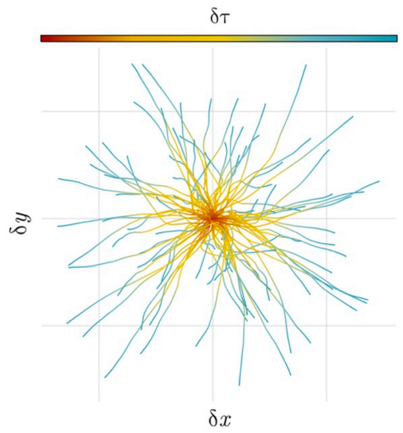

(a) Trajectories in the transverse plane

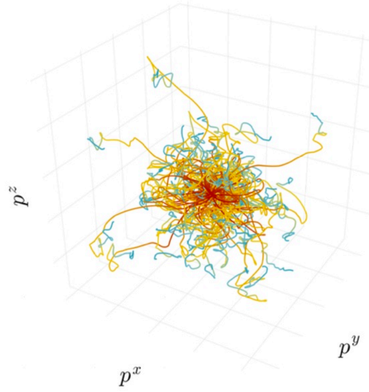

(b) Trajectories in momentum space

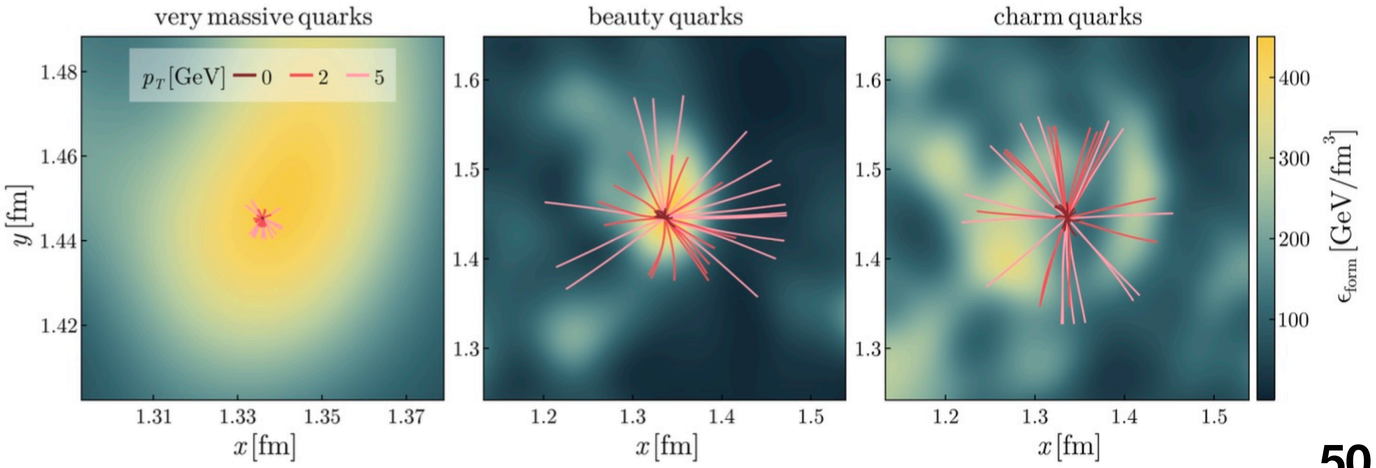

Many other intriguing physics

- ❖ Impact parameter dependence: UPC
- ❖ Sudakov effect vs. Saturation effect: Higgs, Dijet, Quarkonium
- ❖ High multiplicity events in small collision system: Ridge, MPI
- ❖ Elliptic flow from saturation domains: CGC vs. Hydro
- ❖ Medium-induced energy loss of hadron and jet in Cold Nuclear Matter
  - Transport coefficient $\hat{q}$ in cold medium could read $\hat{q}L \sim Q_s^2$.
  - My talk at HardProbes2024: "Medium-induced coherent gluon radiation and heavy flavor suppression in pA collisions", 09/24/2024

Thank you!

Appendix

Cold Nuclear Matter effects

- Heavy quarkonia (J/ψ, $\Upsilon(nS)$,…) as multimeter on QCD/QGP medium in heavy-ion collisions.
- We must peel off Cold Nuclear Matter effects from the data to see genuine QGP.

CNM effects on the market:

- Nuclear parton distribution functions (initial)
- Gluon saturation effect (initial)
- Energy loss effect (initial & final)
- Multiple scattering (Cronin effect) (initial & final)
- Comover (final)
- Nuclear absorption (final)

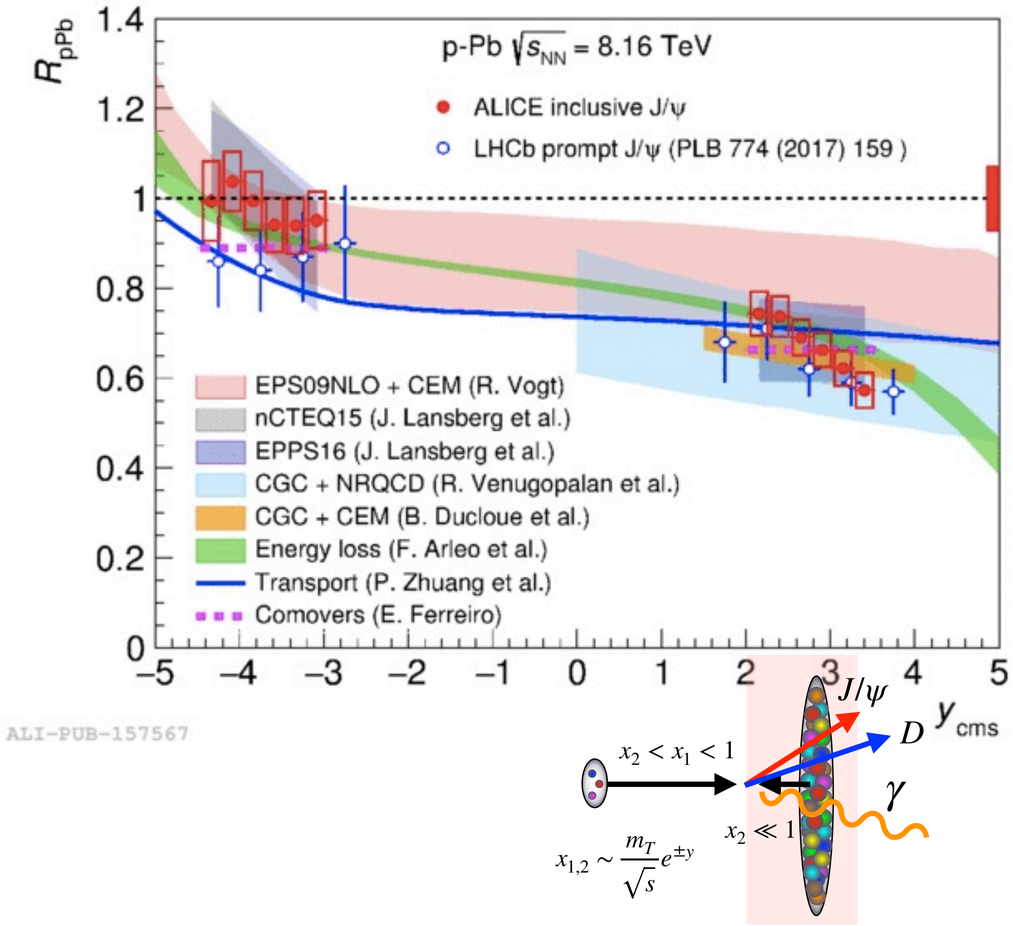

Other observables

LHCb collaboration, [arXiv:2205.03936 [nucl-ex]].